The impact of power management strategies and module sizing for offshore wind turbine integrated electrolysis

T.P. Philippo

Master of Science Thesis

TU Delft

Master of Science Thesis

The impact of power management strategies and module sizing for offshore wind turbine integrated electrolysis

by

T.P. Philippo

To obtain the degree of Master of Science in Sustainable Energy Technology
at Delft University of Technology
To be defended publicly on Wednesday, February 15, 2023 at 9:00 AM.

Student number:	4450698	
Project duration:	March 1, 2022 – February 15, 2023	
Thesis committee:	Dr. ir. M. B. Zaayer,	TU Delft, supervisor
	Ir. O. M. Sane,	Shell, supervisor
	Prof. dr. D. A. von Terzi ,	TU Delft, thesis committee
	Prof. dr. A. J. M. van Wijk ,	TU Delft, thesis committee

This thesis is confidential and cannot be made public until February 15, 2025

TU Delft

Acknowledgements

First of all, I would like to express my deepest gratitude to my supervisors Michiel Zaayer and Omkar Manmohan Sane, for their relentless support, guidance and encouragement throughout my thesis journey. Their valuable insights and expertise have been fundamental in shaping the direction and outcome of my research. I am deeply grateful for the countless hours they spent reading and commenting, providing constructive feedback and challenging me to think critically about my own work. I would not have been able to complete this work without their contribution. Thank you so much for everything.

This endeavour would not have been possible without Omkar, thank you for your trust and the opportunity to perform this thesis at one of the key players in the energy transition. This journey at Shell developed me in several ways and I look forward to starting my career in this company.

Furthermore, I would like to extend my genuine thanks to the members of the thesis committee, Dominic von Terzi and Ad van Wijk. Their assistance with this project and our discussions have been very helpful and guided me in the right direction.

Louis da Costa, thank you for being my sparring partner with modelling in Matlab and for your critical questions towards my modelling and reasoning.

Finally, I want to express my appreciation to my family and friends who have always stood by my side. Their support, confidence and trust have been a constant source of motivation, which keeps me going even during the most challenging times. I am thankful for the numerous times they spent listening to my ideas and helping me to stay focused on my goals. Again, thank you so much for everything.

T.P. Philippo
TU Delft, January 2023

Abstract

Solar and wind will displace fossil fuels as the main source of energy in a net-zero world. However, renewable energy sources provide intermittent power, hence an energy carrier that enables the balancing of demand and supply is needed. Here green hydrogen, created from renewable electricity and water electrolysis comes in place. In addition, green hydrogen assists in transforming the hard-to-abate sectors like the steel industry, aviation, fertilisers etc. to de-carbonise. The demand for green hydrogen is expected to rise in the coming decades. According to IEA, the hydrogen demand will increase from 94 million tonnes (Mt) in 2021 to 530 Mt in 2050 to reach the net-zero scenario. In order to meet the demand, it is essential to create a stable supply. Given the geographical wind resource availability combined with supportive policy, the supply of green hydrogen can be delivered through offshore electrolysis. Moreover, in addition to higher yield, going further offshore creates a stronger case for hydrogen export as power export would become impracticable. The energy industry is investigating what kind of typology and system configuration is most suitable for offshore green hydrogen production. This report provides insight into the performance of a single wind turbine integrated electrolysis system. For which the effect of different control strategies, electrolyser dimensioning and electrolyser capacities are analysed.

The study comprehends the requirements for transforming a single wind turbine into decentralised hydrogen producing wind turbine. This configuration is designed for an offshore application, but is not restricted to an offshore location. This novel system is equipped with a power conversion system, to power the electrolyser and auxiliaries. Seawater lift with water treatment for desalination and demineralisation. And of course, the electrolyser with accompanying balance of system. The BoS covers hydrogen separation and hydrogen treatment. This study selects a PEM electrolyser with three parallel modules of 5 MW capacity each. The individual components are separately modelled and combined to complete the system into a mathematical model. Furthermore, a power management strategy is included. The power management strategy determines which, how much and how many modules are powered. The enhanced results are measured by key performance indicators, which are total annual yield, number of start-stop events and power fluctuation within a module. These KPI's are inspired by the drivers of Shell to get the lowest levelised cost of hydrogen. More hydrogen production drives down the costs and the two other KPI's ensures less degradation on the modules, therefore extending the longevity. Consequently, resulting in lower LCoH.

With the model in place, insights into a decentralised offshore hydrogen producing wind turbine are developed. The goal of the model is to determine which strategy is the best in regard to the KPI's. Furthermore, showing the effect of changing the module sizes and lastly assess the effect of over- and under-sizing the electrolyser capacity. In addition, the model gives insight into the performance degradation for various situations.

This report shows that the use of a power management strategy improves the annual yield, but is also capable of minimising the effect of degradation caused by start-stop events and power fluctuation. This is an important development for improving green hydrogen production, as these strategies can be applied to multiple applications. The equal power division strategy increases the annual yield by at least 2%. The total number of power fluctuations can be significantly reduced by using the segmented start strategy. Finally, a strategy is developed to enhance the longevity of the system and diminish the degradation of the modules. Furthermore, it is recommended to use the three times 5 MW configuration. This configuration achieves the highest performance on the predetermined KPI's. In addition, oversizing of the electrolyser capacity results in under-utilisation of the electrolyser. While under-sizing the electrolysis capacity leads to an increase in performance as the system is utilised more efficiently.

Contents

Nomenclature

Abbreviations

Abbreviation	Definition
AC	Alternating Current
AEL	Alkaline electrolysers
B2B	Back to Back
BES	Battery Energy Storage
BoP	Balance of Plant
BoS	Balance of System
CAPEX	Capital Expenditures
DC	Direct Current
DD	Direct Drive
DFIG	Doubly-Fed Induction Generators
ED	Electro-Dialysis
HHV	Higher Heating Value
HVAC	High Voltage Alternating Current
HVDC	High Voltage Direct Current
IGBT	Insulated-Gate Bipolar Transistor
ISA	International Standard Atmosphere
KOH	Potassium hydroxide
KPI	Key Performance Indicator
LCoE	Levelised Cost of Electricity
LCoH	Levelised Cost of Hydrogen
MSF	Multi-Stage Flash
MED	Multi-Effect Distillation
MVC	Mechanical Vapour Compression
OEM	Original Equipment Manufacturers
OPEX	Operating Expenditures
OSS	Offshore Sub Station
PEM	Polymer Electrolyte Membrane
PEM	Proton Exchange Membrane
PMSG	Permanent Magnet Synchronous Generators
ppm	parts per million
RES	Renewable Energy Source
RO	Reverse Osmosis
SOE	Solid Oxide Electrolysers
SOEC	Solid Oxide Electrolysis Cell
TRL	Technology Readiness Level
WTG	Wind Turbine Generator

Symbols

Symbol	Definition	Unit
v	Velocity	[m/s]
U	Voltage	[V]
I	Ampere	[A]
f	Frequency	[Hz]
P	Power	[W]
A	Area	[m^2]
C_f	Capacity factor	[-]
C_p	Power coefficient	[-]
HHV	Higher Heating Value	[kWh/kg]
B	Status module (1/0)	[-]
Q	Volumetric flow rate	[m^3/h]
H	Height	[m]
g	gravitational constant	[m/s^2]
E	Electric energy	[W]
$\dot{V}_{H_2O}(t)$	Volumetric flow rate	[m^3/h]
W_{des}	Water consumption	[L]
e_{des}	Energy consumption per cubic meter of water	[kWh/m^3]
ρ	Density	[kg/m^3]
η_{module}	Efficiency of module	[%]
$\eta_{degradation}$	Degradation factor	[%]
η_{pump}	Pump efficiency	[%]

List of Figures

List of Tables

1 Introduction

The first chapter contains background information on the general topic and introduces the problem of the research. In addition, it presents the current state of the art related to the topic. After highlighting the problem in the present situation, it motivates the reason for the research. Thereafter, the research objective and additional questions are stated to resolve the issue. Subsequently, the scope of the research and the methodology for solving the problem are defined. Finally, a description of the structure of the report is provided.

1.1. Background information

Concrete actions must take place in the coming years to accelerate the energy transition. One of the key innovations that will help to achieve net-zero emissions is the use of hydrogen. Hydrogen, as an energy carrier, has a crucial role in the energy systems of the future. There are three main reasons: first, hydrogen is preferred to decarbonise hard-to-abate sectors (e.g. steel industry, aviation, shipping and heavy-duty road transportation). Secondly, it enables balancing of customer demand with intermittent renewable energy sources. Thirdly, it is an efficient way to import renewable energy for regions with limited solar or wind potential and helps to reduce the need for grid reinforcements. Therefore, the hydrogen demand will drastically increase over the coming years (IEA, 2022). According to IEA, the hydrogen demand will increase from 94 million tonnes (Mt) in 2021 to 530 Mt in 2050 to reach the net-zero scenario.
To achieve net-zero emissions by 2050, hydrogen must be produced 'green', which means powering water electrolysis with green electrons from renewable energy sources. Considering that the offshore wind sector is facing significant growth and technical advances, hydrogen has the potential to be combined with offshore wind energy to aid in overcoming disadvantages such as the high installation cost of electrical transmission systems and transmission losses. In addition, it is expected that the electrical grid can not keep up with the growth of offshore wind, causing grid congestion. Hence, the direct coupling of wind energy to an electrolyser to produce hydrogen also helps the grid.
The North Sea is the perfect place to produce renewable energy from wind, due to its relatively shallow sea, available space, good connectivity with surrounding countries and with higher mean and more consistent wind speeds. Consequently, this potential can be used for the synergy between wind energy and hydrogen. Hence, the North Sea is appointed to be one of the most promising energy hubs in the world.

There are two logical locations for green hydrogen production namely, onshore or offshore.
To produce onshore hydrogen from offshore wind, Offshore Sub Station(s) (OSS), HVDC cables and/or HVAC cables are needed for the connection to shore. Considering offshore hydrogen production, the hydrogen is produced close to the wind farm and is transported to shore with pipelines. From an economic point of view, the goal is to produce hydrogen for the lowest cost to make it competitive. Thus, the location is based on where the lowest levelized cost of hydrogen (LCoH) can be achieved. Around 60% of the cost of green LCoH is caused by the levelized cost of electricity (LCoE) (IRENA, 2018), meaning that a low LCoE positively influences the LCoH. According to Calado & Castro (2021), the cost of electricity used by the electrolyser placed onshore will be higher in the future than the cost of

electricity used by same-sized electrolyser placed offshore. The main reason for this is the difference in cost and transmission losses of hydrogen pipelines compared to electrical cables. Hence, the scope of this research is offshore electrolysis, where the produced green hydrogen is transported to shore via designated pipelines.
One of the reasons why offshore green hydrogen production is cheaper than onshore production is that the transportation of molecules beats electrons over a long offshore distance (TNO, 2019) (Calado & Castro, 2021). Not only do pipelines have fewer transmission losses (0.1%) compared to cables (5%), but they are also cheaper over long distances and are capable of transporting higher capacities. The cables are more expensive than pipelines mainly due to the production cost and the need for an offshore substation (Miao et al., 2021). However, this does not mean all offshore wind energy should be converted into hydrogen. Nearshore, electricity will be preferred. Although looking forward to the near future with grid congestion, further distanced wind parks and an increasing hydrogen demand, offshore hydrogen production will be inevitable. According to a Shell internal report (Shell, 2018), offshore hydrogen production is preferred over onshore after more than 150 km from shore. Around 100 to 150 km, the CAPEX of both are similar.

Green offshore electrolysis is categorised into three typologies: using an energy island, centralised hydrogen production by use of a platform, or a decentralised solution where an electrolyser is integrated with a single wind turbine. Comparing the CAPEX of each solution, an Energy Island/Hub is the most expensive and is far away from being realised. Furthermore, when comparing centralised vs decentralised, they both have big advantages and disadvantages. However, a decentralised solution is expected to be realised with 20%-30% less CAPEX (Shell, 2021). Besides lower costs, North Sea Energy expects a higher annual hydrogen yield of about 5% with a decentralised solution, because of less conversion losses in the system (North Sea Energy, 2018). Accordingly, producing more hydrogen for the same or lower price. Ultimately, achieving lower LCoH and a stronger competitive case. Additionally, Daniel Fernandes' thesis, which compares centralised onshore, centralised offshore and decentralised offshore hydrogen production, concludes that the in-turbine configuration (referring to an electrolyser integrated into a wind turbine) achieves the lowest LCoH in the North Sea (Fernandes, 2020).
Nonetheless, the OPEX, mainly consisting of operation and maintenance costs, can be the bottleneck for a decentralised solution. There are multiple points of operation and control, so if one of the systems fails, an engineer has to go offshore to fix one stand-alone system, which is costly. To prevent high OPEX, the reliability of the system needs to be high. High reliability is not only beneficial for the LCOH, but also for the electrolyser.
From a public consultation to the Ministry of Economic Affairs and Climate Policy and the Netherlands Enterprise Agency, it becomes evident that experts and electrolyser manufacturers agree that electrolyser degradation occurs under partial and full load, start-stop events and frequent power fluctuations (Rijksdienst Voor Ondernemend Nederland, 2021). However, the effects of degradation are not yet quantified by this group of experts. With an electrolyser directly coupled to a wind turbine, it is expected that the previously mentioned degradation causes will happen more frequently due to the intermittency of the source. The actual causes of cell performance degradation have been studied in detail by Ginsberg et al. (2022). Furthermore, this study suggests some engineering improvements to enable more robust operation of a PEM electrolyser (Ginsberg et al., 2022). However, these solutions reduce the effect of cell performance degradation, but do not prevent the cause. To diminish the cause of cell performance degradation, the number of start-stop events and the number of power fluctuations needs to be reduced. A power control strategy could reduce this. In addition, a power management strategy could also increase the efficiency of operating an electrolyser under an intermittent power source like wind energy.

State of the art of decentralised hydrogen production
Currently, a self-sustaining offshore hydrogen producing wind turbine only exists on paper. However, there are some existing projects that come close to this principle. One of them is the Brande Hydrogen pilot, where Siemens Gamesa produces green hydrogen directly from wind. This onshore turbine can produce hydrogen in "island mode", but can also operate connected to the grid. Another comparable pilot is the Duwaal project, by HYGRO. For this project, HYGRO connects a 4 MW onshore wind turbine directly to an electrolyser, showing that hydrogen can be produced more efficiently from wind energy

directly at the turbine. Similar is the AmpHytrite project by GE, Sif and more. This feasibility study focuses on a centralised offshore and off-grid hydrogen production unit. Here multiple turbines are connected to one electrolyser. A more offshore-focused project is the SEM-REV project by Lhyve. Here, a floating wind turbine is connected to a floating electrolyser. Both are still connected to the grid. Nevertheless, this demonstrator shows that it will be possible to produce hydrogen offshore from a single wind turbine.
Furthermore, ERM is developing a floating hydrogen producing wind turbine called Dolphyn. Their aim is to construct and operate the first 10 MW unit by the end of 2024 (ERM, 2019). All these projects have the same objective in mind, namely contributing to an affordable large-scale offshore green hydrogen production.

1.2. Problem analysis

In order to understand the challenges of an integrated electrolyser with an intermittent power source, more insights into the full system are needed. The lack of insights is caused by the scarcity of extended literature and due to the constraints for manufacturers of being in a product development phase. Consequently, there is no consistency in the ideal system configuration and sizing of the components.
One of the biggest challenges with green hydrogen production is the performance degradation of the electrolyser. One cause for this is the sensitivity to turning on and off frequently. Continuously switching of the electrolysers, causes problems around the diaphragms (gas moves more easily from one side to the other) and at the electrodes (especially at the cathode, corrosion occurs when stopping too often) (Ginsberg et al., 2022). Therefore, increasing the potential loss of performance, increasing crossover risks and increasing the percentage of hydrogen in oxygen at low power. In other words, an increased chance of system failure and of explosions. Hence, a strategy should be developed to diminish the switching times. Another way to prevent crossover is to define a minimal operational power load for the module. However, this is an underexposed part of electrolyser literature. Furthermore, a high fluctuating power supply to the electrolyser also influences the effect of degradation and should be investigated.
Another system challenge is making the system self-sustaining, meaning that it can operate without connection to the grid. Consequently, making the system more resistant to low/no-wind and extreme wind conditions. In these periods normal wind turbines are in standby mode, however, power is needed to pitch and yaw the turbine after the standby period. Therefore, energy storage in the form of a battery or generator should be included in the system just for the wind turbine. The self-sustaining system needs to be capable of doing a black start with grid forming when needed.
To make a self-sustaining hydrogen producing offshore wind turbine more efficient and therefore more cost-effective, a power management strategy is needed to optimise performance. Currently, control strategies for powering electrolyser modules are of limited knowledge and under strict custody by original equipment manufacturers. Foremost, there is an absence of good models about the performance life of an electrolyser, regarding the effect of switching, handling with intermittent wind power and degradation over time. Moreover, no optimisations for yield, switching times or power fluctuations for an electrolyser are found in the literature. Therefore, extended insights are needed into degradation management and degradation modelling of the electrolyser coupled to intermittent power sources.
The challenges above will help to form the research objective, accordingly, the associated research questions are assembled. The research objective and questions are listed below in the next section.

1.3. Research objectives and questions

The objective of this study is to provide insight into the performance of an offshore hydrogen producing wind turbine, analysing the effect of different control strategies and electrolyser dimensioning. The associated research questions below support achieving this research objective.

- Which strategy achieves the highest performance?
- What is the effect on performance by changing the total number of modules?
- What is the effect of over- and under-sizing of the electrolyser capacity with a fixed wind turbine size?

1.4. Research boundaries

The scope of the project is to combine an offshore wind turbine with an electrolyser and all necessary equipment, to create hydrogen solely from the power produced by the wind turbine. This technology solution shall be able to produce hydrogen without any support from the electrical grid and be self-sustained. Therefore, the scope is limited to one single wind turbine electrolyser configuration.
The scope covers the system configuration, component selection, electrolyser module dimensioning, comparing different electrolyser capacities and adequate strategies. Because the scope is on a single wind turbine electrolyser combination, no wake losses of close-by wind turbines are considered. The same counts for the wake losses of adjacent wind farms. The decentralised hydrogen turbine will be located on the North Sea, within the Dutch sea borders.
The hydrogen producing wind turbine is designed to only produce hydrogen as an output, thus the possibility of a hybrid form (electricity and hydrogen) is not considered. For a decentralised configuration, it is possible to go with a floating wind turbine. However, floating wind turbines are still in their infancy and need a higher Technology Readiness Level (TRL) for commercial deployment. Besides, placing a fragile electrolyser on a moving platform brings additional challenges, which are underexposed in literature. Therefore, the scope includes a fixed offshore wind turbine and excludes a floating design. The different possible foundations and installation of the configuration, will not be taken into account in this research.
The scope will only include high TRL electrolyser and desalination technologies. The final part that is covered in the scope is gas purification, therefore the scope of the report ends before hydrogen transportation. Hence, any needed risers and pipelines with their pressure fall will not be considered. Consequently, compressors and manifolds will not be included in this study. Moreover, oxygen will be vented after separation.
The effect of dynamic loads and vibration of the wind turbine on the system, are not considered. However, this could be of importance for future research.

1.5. Methodology

This section highlights the methodology used to answer the research objective and questions.
First, a thorough literature study has been executed to gain an understanding of the existing research, investigate state-of-the-art technologies and identify any research gap. The literature study focuses on different aspects, like offshore hydrogen production, hydrogen production from renewable energy sources and electrolyser modelling. After which the research scope and objective are defined.
From this research, a general system design is selected and possible components of the system are identified. The goal is to have a realistic system configuration with the selected components. The system configuration is based on combining existing proven technology and applying it for use in a novel way. This means that a single fixed offshore wind turbine will be directly coupled to an integrated electrolyser with all auxiliaries required, the so-called balance of plant. Afterwards, the possible components are compared and the most suitable are selected to fill the general system configuration. When all components are integrated with detail, the initial sizing of components is done. The dimensioning of system components is done in a pragmatic way: a reasonable design, but not necessarily optimised.
For each selected component, the characteristics, mathematical equations and their relationship with other components are collected. Eventually, all information on the selected components is gathered together in a high-level model. Creating a robust high-level model of the system helps to understand the system's behaviour. The mathematical model is used to simulate wind energy and hydrogen production based on smart switching. The power demand of the system is determined by real-time hourly wind speed data. The model will be completed with all dynamic equations of the system and is explained in more detail.

The next step in the methodology is to design a control strategy for yield, switching times and power fluctuation in a module. Consequently, key performance indicators (KPI's) are defined to measure the system's performance. These KPI's are intended to validate and compare the performance of the different strategies. The designed KPI's are also used to clarify the difference in various configurations of the electrolyser modules.
The function of the strategy is to control the load demand of the electrolyser and its balance of plant. Therefore utilising the available power in the best way. With the mathematical model in place, various

dimensioning of the electrolyser are analysed. This results in the possibility to compare different module sizes with the same electrolyser capacity, but also to analyse the effect of over- and under-sizing of the electrolyser capacity with a fixed wind turbine size.
With all the possible dimensioning and strategies, several case studies are defined. Here the possible configurations are combined with one of the strategies and the outcomes are compared. This is all done for the same wind year input data for a fair comparison. After a year of operation, the different cases are compared on their performance with the KPI's. Besides, the model also shows the effect of degradation on the modules. Which shows if a strategy has a positive or negative influence in the long run. Accordingly, an analysis is done to get a comprehensive understanding of the system dynamics, performance, scale, losses and efficiencies.
As a final assessment, the different configurations and strategies are tested on different scenarios. In this sensitivity analysis, the system is subjected to low-wind conditions from another year, but same location. Next to that, the electrolyser parameters are modified to analyse the effect.

1.6. Report layout

The report is structured according to the sequence outlined in the methodology section. After the introduction, Chapter 2 presents an overview of the system configuration. Chapter 3 provides the components selection of the system configuration. With the knowledge of both the configuration and components, the mathematical model is developed and outlined in Chapter 4. The results of the model are presented and analysed in Chapter 5. The validity of the results is verified through a sensitivity case study in Chapter 6. Finally, Chapter 7 concludes the research study by summarising the main findings and implications.

2

System configuration

The system design of a decentralised off-grid hydrogen producing offshore wind turbine is derived from the idea to produce hydrogen at turbine level. To support the electrolyser and its balance of plant, a dedicated newly designed platform will be attached to the wind turbine. The platform on which the system is housed will be similar but bigger than a service platform. A conceptual layout of the system is visualised in Appendix F. The system consists of modular design blocks, e.g. the modular components for electrolysers and a modular component to hold auxiliary systems. The system design includes electrolyser stacks, electrolyser's balance of plant, seawater intake and desalination, and a power conversion system. Figure 2.1 below, shows the complete general configuration of the system.

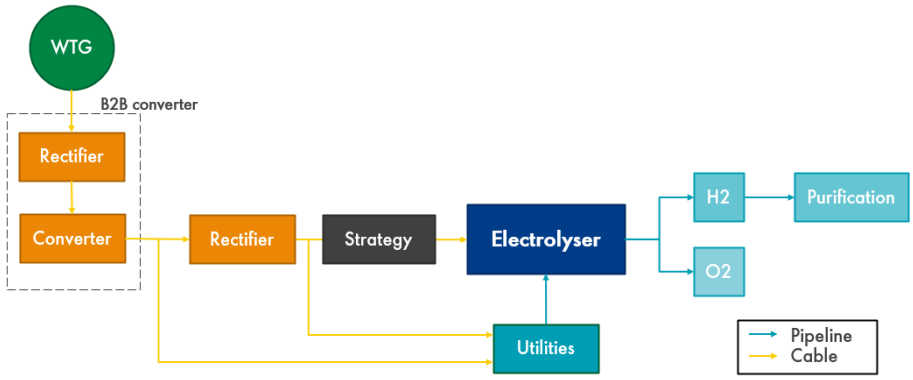

Figure 2.1: General system configuration for a decentralised offshore hydrogen producing wind turbine.

A key advantage of a decentralised solution, compared to centralised is the possibility of optimising the electrical architecture of the configuration. With this optimised configuration a lower CAPEX, lower power losses and therefore higher yields can be achieved. The comparison between the conventional connection and the optimised connection is pictured in figure 2.2. The conventional configuration is the top figure, here the general power conversion from a wind turbine is unchanged. Hence, after the generator, a back-to-back converter is positioned. This back-to-back converter put the output in a $50Hz$ frequency, which is needed for the grid (Madariaga et al., 2012). After the back-to-back converter, the transformer converts the output to HVAC. HVAC is used because of the easier and cheaper step-up/step-down conversion (May et al., 2016). However, the electrolyser operates with low to medium-voltage DC power. Therefore, an additional transformer and rectifier are needed. Looking at the optimised electrical architecture below, all the unnecessary components are removed. Improving the connection between the generator and the wind turbine. Note that for auxiliaries in the optimised configuration a converter and transformer are needed, however, this is not depicted in the figure. More details on the electrical configuration and components are discussed later in the report.

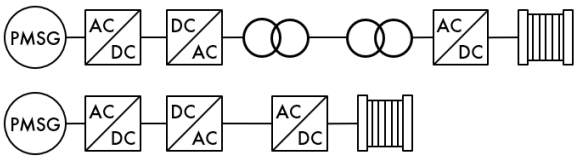

Figure 2.2: The comparison of the conventional (above) en optimised electrical architecture (below). Showing the direct connection between the Permanent Magnet Synchronous Generator of the wind turbine and the electrolyser. Electrical architecture for auxiliaries are excluded in this figure.

With respect to the system configuration, the ratio between electrolyser capacity and turbine capacity is not fixed, but is a design parameter. In this report the turbine size is fixed, therefore the electrolyser capacity is modified to show the effect of over and under-sizing. Another design parameter is over how many modules the electrolyser capacity can be divided. These different design parameters are analysed in different cases and are discussed later in the report.
In the next chapter, all components of the system will be discussed in more detail as to why they are selected for the system design.

3

Component selection

Chapter 3, discusses which components are used in the final system configuration. Different technologies are compared to each other to have a fair component selection. The chapter starts with the most important component, the electrolyser. Afterwards, the power conversion, water intake and water treatment are discussed.

3.1. Comparing Electrolyser Technologies

Water electrolysis is a process in which electrical energy is used to split water molecules into hydrogen and oxygen. The process can be carried out using an electrolyser, which typically consists of two electrodes (an anode and a cathode) and a source of electrical energy. The anode and cathode are usually made of a conductive material such as platinum or carbon. When an electric current is passed through the electrolyser, the water molecules at the anode are oxidised to form oxygen gas and hydrogen ions. At the cathode, the hydrogen ions are reduced to form hydrogen gas. The process can generally be described by the equation: $2\ H_2O\ +\ electricity \rightarrow 2\ H_2 + \ O_2$ (IRENA, 2020). Electrolysis technology has improved significantly over the past decades. The three main electrolyser technologies are Alkaline, Proton Exchange Membrane and Solid Oxide Electrolysers. The key characteristics of these technologies are summarised in table 3.1.

Alkaline electrolysers (AEL) were the first commercially deployed electrolysers and have been used by the industry for almost a century. During this time, it has been applied for large-scale (MW-scale) hydrogen production and has proven a track record for operational performance and reliability (IRENA, 2018). In an alkaline electrolyser, the electrodes are immersed in a liquid electrolyte separated by a diaphragm. The most commonly used liquid electrolyte is Potassium hydroxide (KOH), with a 25–30% aqueous KOH-solution. This liquid electrolyte is used for avoiding corrosion problems caused by acid electrolytes (Santos et al., 2013). However, the use of a liquid electrolyte increases the chance of leakage and therefore the need for maintenance (ERM, 2019). This brings additional challenges and costs when placed in an offshore environment. According to Ibrahim et al. (2022), liquid electrolyte has a relatively limited response to fluctuations from electrical inputs. Especially the response to sudden changes in the power supply, like a complete stop or a peak is noticeable. This adds more challenges, given that wind turbines have a highly variable electrical output. Various research papers have investigated the increase in the compatibility of AEL to fluctuating input current. They expect that the compatibility of AEL coupled with a renewable energy source will be more commercially mature in the near future (David et al., 2019) (Ibrahim et al., 2022). The operational pressure in an AEL is usually limited to 30 bar, hence it may require additional compression to enable export through pipelines to shore (ERM, 2019).

The Solid Oxide Electrolyser (SOE) or Solid Oxide Electrolysis Cell (SOEC) technology has gained increasing attention because of its promise for high efficiencies. However, SOEC is a less mature technology and has only been deployed at laboratory and small demonstration scale (IRENA, 2018). The biggest difference with other electrolyser technologies is that SOEC requires a high-temperature

source to operate and uses a ceramic membrane. Due to the high-temperature operation, it is difficult to switch the system on and off (Geerlings & Mulder, 2021). The high temperature also brings the challenge for material stability (Buttler & Spliethoff, 2018). For a high-temperature source offshore, an additional system is needed. It is expected that this will increase the footprint, complexity and the CAPEX of the plant. Whilst the technology is believed to have potential, it is not considered for offshore application in this study. However, SOEC may prove to be an advantageous technology for other systems in the future.

Proton Exchange Membrane (PEM) or Polymer Electrolyte Membrane (PEM) electrolysers use a solid polymer electrolyte, which isolates the anode from the cathode but closes the electric circuit. PEM electrolysers use expensive catalysts made from noble metals such as platinum (at the cathode side) and iridium (at the anode side), which increases the cost of the electrolyser (Ibrahim et al., 2022). However, PEM has the highest Technology Readiness Level (TRL), namely 7–8, when it comes to coupling with a dynamic electric input, like a Renewable Energy Source (RES) (Hernández-Gómez et al., 2020) (Schnuelle et al., 2020). The PEM electrolyser has a rapid response to fluctuations in electrical input, which is critical for direct coupling with a decentralised offshore wind turbine (Buttler & Spliethoff, 2018). The efficiency of a PEM electrolyser depends on several factors and is different for each manufacturer. To give an example, in 2020, Siemens Energy achieved efficiencies of 75.5% and higher with their 17.5 MW PEM electrolyser system “Silyzer 300” (Siemens-Energy, 2020). One of the major advantages of PEM compared to other electrolysers, is that it features shorter start-up times, especially from cold operating temperatures (Buttler & Spliethoff, 2018). Next to that, due to a solid polymer and a high current density operation, PEM has a relatively compact system design. This is preferable when spacing becomes a constraint (Ibrahim et al., 2022). Furthermore, the electrolyser is able to produce pressurised hydrogen of 30-50 bar (Buttler & Spliethoff, 2018). At this pressure rate, it could be possible to export the hydrogen to shore without the need for an additional export compression system (ERM, 2019) (e.g. a reciprocating compressor). The last advantage over other electrolysers is, by the use of a solid membrane, there is less cross-permeation, therefore yielding hydrogen of higher purity (>99%) (Buttler & Spliethoff, 2018). In addition, solid membranes achieve lower minimal load levels compared to other electrolyser technologies.

	AEL	**PEM**	**SOEC**
Operating parameters			
Cell temperature (°C)	60-90	50-80	700-900
Typical pressure (bar)	10-30	20-50	1-15
Flexibility			
Load range (% of nominal load)	20-100	0-100	30-125
Efficiency			
Nominal system efficiency (HHV)*	62-82	60-80	73-85
Capacity			
Maximal nominal power per stack (MW)	6	2.5	<0.01
Durability			
Lifetime (x1000 h)	55-120	60-100	8-20
Degradation (%/year)	0.25-1.5	0.5-2.5	3-50

Table 3.1: Overview of characteristics of water electrolysis technologies (Buttler & Spliethoff, 2018) (Singlitico et al., 2021) (Siemens-Energy & Lettenmeier, 2021) (IRENA, 2020). *System efficiency including the energy consumption of the electrolyser stacks, gas water separators, gas drying, water management, electrolyte system (for AEL), system control and power supply.

Selecting the electrolyser and its balance of plant

As mentioned above, the SOEC is unsuitable for a decentralised hydrogen producing wind turbine. However, alkaline and PEM are both suitable. Hence, the advantages and disadvantages of each technology are compared. Table 3.2, shows the pros and cons of both electrolysers. Due to the thin membrane of the PEM electrolyser, there is a lower resistance, resulting in a higher current density. Next to that, higher voltage efficiencies can be achieved.

	Advantages	Disadvantages
PEM	Thin membrane Low corrosion Good switch-ability Small footprint Fast start-up Simple maintenance Good partial load range Dynamic operation High purity	Requires noble materials Costly Short lifetime Possibly low durability Acidic corrosive environment
AEL	Relative low cost Higher durability Well established technology Stacks in MW-range	Caustic electrolyte Bulky Slow response to fluctuating power Slow start-up Low operational pressure Many components Complicated maintenance Crossover of gases

Table 3.2: Table for the comparison of pros and cons of AEL and PEM electrolyser technology (Guo et al., 2019) (Hernández-Gómez et al., 2020) (Schnuelle et al., 2020) (Buttler & Spliethoff, 2018) (David et al., 2019) (Siemens-Energy & Lettenmeier, 2021) (Geerlings & Mulder, 2021) (Santos et al., 2013).

Based on the pros and cons in table 3.2 and the challenges that come with direct coupling with a wind turbine, PEM is selected as the best suitable electrolyser technology.
The selection of PEM is based on three key factors. First, a complete PEM electrolyser system has a smaller footprint and weight compared to AEL and SOEC. Therefore, the PEM electrolyser is more suited to offshore use, as space is limited and the system needs to be containerised for marine protection. A rule of thumb in the offshore industry is, more weight adds to more cost.
Secondly, the PEM electrolyser is better able to coop with high fluctuating power input, according to Hernández-Gómez et al. (2020) and Schnuelle et al. (2020). As wind speeds vary over time, this is an important characteristic. Fluctuating power also influences the degradation rate of the module, which is not beneficial when operated in remote offshore areas.
Thirdly, PEM produces hydrogen under pressure up to 30-50 bar (Buttler & Spliethoff, 2018). Producing hydrogen under pressure decreases the need for compressors as the hydrogen needs to be transported to shore. Eliminating the need for an additional export compression system reduces the cost and complexity of the system.
In conclusion, a PEM electrolyser is used in combination with the turbine, due to its compactness, fluctuating power capabilities, high output pressures, good efficiencies and low minimal load requirement.

Figure 3.1 shows the generic system of a PEM electrolyser. As can be seen, the system consists of three parts: power conversion, electrolyser, Balance of System (BoS). The system flow is simple (and similar for all types of electrolysers). However, this may differ per manufacturer, size and purpose. The system starts with a connection to a power source, which can be the grid or a renewable power source. Depending on the power source, the power needs to be converted to the right specifications for the electrolyser. Despite the origin of the electrons, the electrochemical stack can start operating and split the supplied water into hydrogen and oxygen. After the production of these gasses, the gasses need to be separated. Finally, the gas is purified with a deoxidiser (extract excess oxygen from the hydrogen) and a drier (extract leftover water from the hydrogen) and is now ready for export.

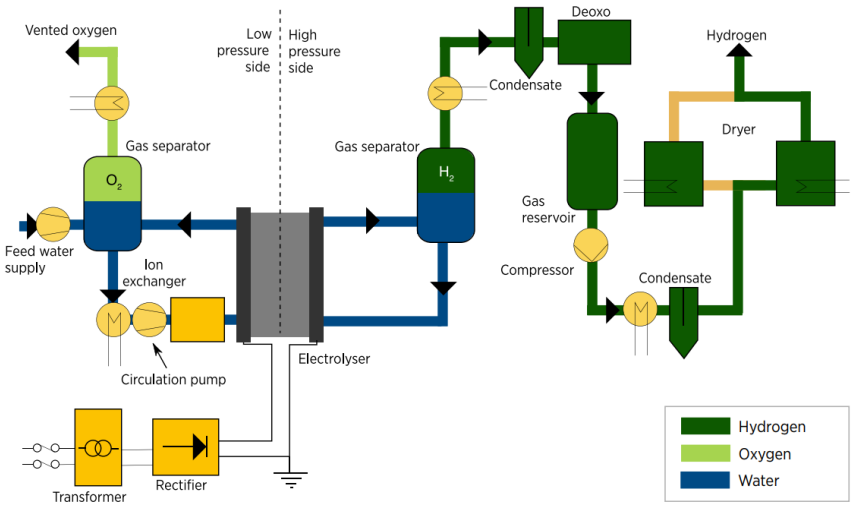

Figure 3.1: Typical system design and balance of plant for a PEM electrolyser (IRENA, 2020).

3.2. Wind Turbine

For this study, the electrolyser is combined with the novel reference IEA 15 MW wind turbine (NREL, 2020). Despite not being a real component selection, but more a conceptual choice, the turbine is selected to keep the case study generic. In addition, the IEA 15 MW Reference wind turbine is selected, because of the expected growth in size for the offshore wind industry. It is suitable for large-scale wind energy projects due to its standardised design, which can be used as a benchmark for comparing the performance of other wind turbines. The turbine is designed to operate in a wide range of wind conditions, including both low and high wind speeds, making it a versatile design. Additionally, the turbine is designed to be highly reliable, with a low level of maintenance required, which helps to keep operating costs low. Furthermore, the turbine is designed with the latest technology, making it more efficient and therefore more productive (NREL, 2020).

The wind turbine is equipped with a direct drive generator. The most important characteristics of this wind turbine are shown in table 3.3. The typical power curve is shown in figure 3.2, where it is important to notice the shape of the curve. The boundaries of the curve are determined by the cut-in and cut-out speed, the shape by the cubic wind energy formula and the plateau by its rated power. The formula to create the power curve is shown in the next chapter.

It is assumed that this wind turbine possesses the newest innovations, which makes the turbine self-sustaining and capable of performing grid forming and black starts. A self-sustaining wind turbine provides mitigation against the negative consequences of off-grid situations. This is done with the use of a back-up power source and multiple operational modes for the turbine. The back-up power provides energy to the turbine and the turbine's auxiliaries, when there is no power produced. The back-up power will only support the wind turbine power needs and not of the electrolyser. Therefore the back-up power system is not a design parameter in this study.

The purpose of grid forming, when connected to the grid, is to positively influence grid stability. This is done by a control strategy of the wind turbine generators (WTGs). In contrast, currently used standard wind turbines are controlled by a "grid following" method. Grid forming also enables black starts. A black start is the process of restoring (a part of) an electric grid to operation without relying on an external electric power network to recover from a total or partial shutdown. Meaning that the local system grid is restored to power the electrolyser and balance of plant after a period of no power generation.

These two innovations together, enable the turbine to produce electricity and therefore hydrogen off-grid. Siemens Gamesa Renewable Energy calls this 'island-mode' and is currently testing this strategy with the project Brande Hydrogen (Siemens-Gamesa, 2021).

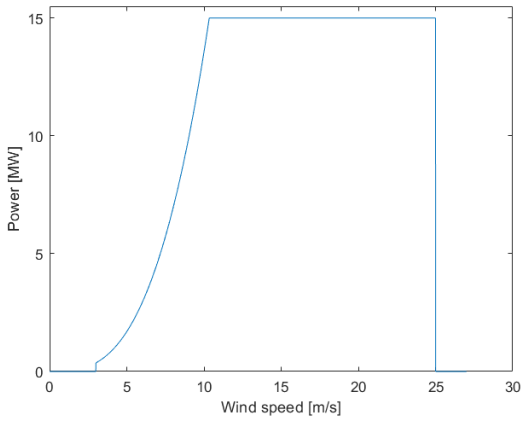

Figure 3.2: Power curve of the 15 MW IEA reference wind turbine.

Parameters	Value
Rated power [MW]	15
Cut-in wind speed [m/s]	3
Rated wind speed [m/s]	10.6
Cut-out wind speed [m/s]	25
Rotor diameter [m]	240
Hub height [m]	150
Drivetrain [-]	Direct drive

Table 3.3: Key Parameters for the IEA 15-MW Turbine (NREL, 2020)

3.3. Power Conversion

The generator inside the nacelle produces electrical power from wind energy. There are two common types of generators for wind turbines: doubly-fed induction generators (DFIG) and permanent magnet synchronous generators (PMSG). A typical wind turbine is equipped with an AC Direct Drive PMSG. The wind turbine produces medium-voltage AC power. As shown in figure 2.2, for the electrolyser to utilise this power a rectifier is placed in between. The rectifier converts the AC power into DC power. The AC power generated by the generator is connected to an AC bus bar, so components like the seawater intake that work on AC power can consume the AC power directly. Furthermore, auxiliaries that operate on DC power, receive their power from the DC bus bar. This bus bar is powered by the rectifier before the electrolyser.

Comparing the power conversion of a standard wind turbine, the most used configuration is respectively: a generator, AC/DC converter, DC/AC inverter and a transformer (Nejad et al., 2022). The AC/DC/AC conversion is also known as a back-to-back converter. This output AC power can be connected to the grid. However, if the distance to shore is large, then it is advised to use an Offshore Sub Station (OSS). An OSS is an inter-array cable connecting point of a platform, where the incoming AC power is converted to high-voltage DC power to reduce power losses during transportation (May et al., 2016). Once arrived at shore, the DC power will be converted back to AC for grid connection.

3.3.1. Rectifier

Depending on the type of wind turbine generator (WTG) and its output, the system may need to use diode-based AC/DC rectification converters. The typical wind turbine produces AC power from a direct drive generator, therefore the use of a rectifier is inevitable as the electrolyser requires DC input power. Each module is equipped with a rectifier and the electrical losses are accounted for in the efficiency curve of the electrolyser. However, some equipment of the system requires DC power (e.g. desalination and batteries).
The most common AC/DC converters used in large-scale industrial applications is the three-phase

bridge rectifier and the Insulated-Gate Bipolar Transistor (IGBT). The advantage of an IGBT active rectifier is that the filtering section reduces harmonic distortion to an acceptable level. This ensures smooth running of the system and is, therefore, most likely used in the electrolyser (Ayodele & Munda, 2019).

3.3.2. Transformer

The electrolyser is able to follow the fluctuating voltage of the generator, however, this fluctuating effect can damage other equipment. The transformer is coupled to AC power and transforms the voltage to a lower level around 400-690V. The transformer is connected to an AC bus-bar, from this power line AC power auxiliaries are operated.

3.4. Water System

The water system consists of the process of collecting seawater and desalinating seawater into fresh water for hydrogen production. These parts are covered in the following sub-sections.

3.4.1. Water Intake

Key to hydrogen production is the supply of water, also called feed water. The best way to supply water in a remote location at sea, is to use seawater. This water is lifted with a pump from below the sea surface to the platform. The water intake has a filter to prevent wildlife or dirt from entering the system. The seawater is processed into usable feed water later in the process.

3.4.2. Water Treatment (Desalination)

For electrolysis, the water in the process needs to be of high purity (<5 ppm). However, seawater contains a lot of impurities like salt. This salt needs to be extracted from the water before electrolysis. This section discusses the possible options for desalination and selects the preferred component. The selected component is described in more detail in the next chapter for modelling. There are several types of desalination units, which are divided into two technologies: thermal (phase-change) processes and membrane processes. However, the most conventional desalination processes which operate on a thermal distillation technique (e.g. Multi-Stage Flash (MSF), Multi-Effect Distillation (MED) and Mechanical Vapour Compression (MVC)) are bulky systems and require thermal energy like steam. These are undesirable characteristics for a decentralised offshore off-grid solution. It could be feasible but, converting power into steam has a low energy efficiency. Therefore, a desalination process that efficiently runs on electrical power is preferred. So, a membrane process will be selected.
There are two well-developed membrane desalination technologies, Electro-Dialysis (ED) and Reverse Osmosis (RO). Electrodialysis is an electrochemical separation process that operates at atmospheric pressure and uses DC to move salt ions selectively through a membrane, leaving fresh water behind (Al-Karaghouli & Kazmerski, 2013). ED produces fresh water with less electrical energy, however, the operational capacity of the process is the lowest of all desalination units (Al-Karaghouli & Kazmerski, 2013). In addition, ED works better with brackish water instead of seawater. Hence, this technology is not selected.
The final desalination technique is Reverse Osmosis. RO is a widely available and trusted technology with a low energy consumption and capable of processing high capacities of seawater. According to Khan et al. (2021), RO and PEM are an ideal couple for the lowest LCoH and best performance (Khan et al., 2021). In conclusion, this technology has low energy requirements, a small equipment footprint and low CAPEX compared to alternative technologies. Consequently, Reverse Osmosis (RO) is selected as the most suitable desalination technology. Hence, this technology is treated in more detail below.

Reverse Osmosis (RO) is a form of pressurised filtration with a semi-permeable membrane. This filter allows water to pass through, but not salt. This yields permeated fresh water and leaves highly concentrated salt water, called brine, on the high-pressure side of the membrane (Al-Karaghouli & Kazmerski, 2013). Figure 3.3, shows a schematic diagram of an RO system. Before entering the high pressure pump, the seawater is pre-treated. Here the seawater is already treated with filtration and chemicals are injected to prevent scaling and bio-fouling. The post-treatment removes any unwanted gasses from the fresh water. Reverse osmosis technology is a proven desalination technology and is

already applied on large scale in the offshore industry. However, there is one downside to RO compared to other technologies and that is that it requires more maintenance visits for cleaning or replacing the membranes. This adds high OPEX costs to the system.

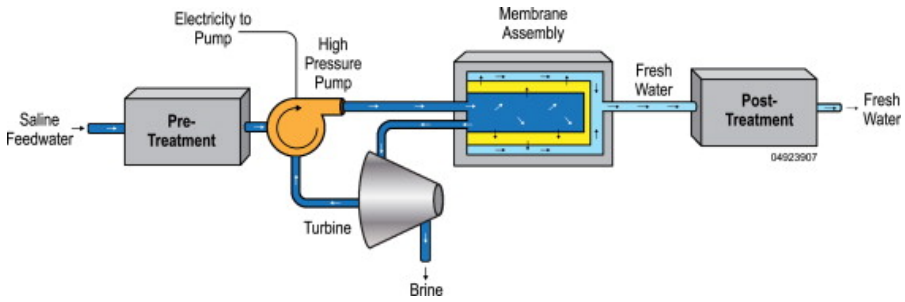

Figure 3.3: Schematic diagram of a Reversed Osmosis system (Al-Karaghouli & Kazmerski, 2013).

4

Modelling of the system

This chapter gives an elaborate overview of the modelling used to describe the complete system. First, the model is analysed from a helicopter view and the key performance indicators are explained. The second section describes the wind input data. Here suitable wind data is selected and the modelling of the turbine is described. The third section, explains the heart of the system. Here the electrolyser and balance of plant modelling are described in detail. In the fourth section of this chapter, the functioning of different strategies is explained. Finally, the possible module configurations are explained.

4.1. Model explanation, assumptions and implementation

The goal of this model is to understand the component and system behaviour under various wind conditions. Additionally, the model gives an extensive insight into a wind-to-hydrogen system. Furthermore, the model shows the effect of using diverse strategies and the effect of various configurations of the modules. Moreover, the model is capable of showing the effect of having a different electrolyser capacity compared to a fixed wind turbine size. The difference in performance is measured in key performance indicators, which are explained in chapter 4.1.2. Consequently, the aim of this model is to support answering the research questions which are defined in section 1.3.
The model is created in MATLAB and consists of multiple self-made functions to support the script.

4.1.1. Overview of the system's model

A block diagram of the system model is shown in figure 4.1. It provides an overview of the steps made in the model. The model starts with hourly wind data from a selected year and is then combined with the power curve of the 15 MW IEA wind turbine. At this point, we know the wind turbine performance, which is key to the system. All the power generated by the wind turbine will be used to create as much hydrogen as possible. However, the auxiliaries and the BoP consume a part of the available power. This is accounted for in the system losses, which mainly consist of power conversion losses, auxiliaries losses and losses from the water lift and treatment. Depending on the available power and the selected strategy, the model calculates how much hydrogen can be produced.
To produce 1 kg of hydrogen, 10 litres of purified water is needed. This water is purified seawater, which is processed by the system. This process also consumes electricity, therefore these losses are accounted for in a feedback loop. This will be explained in more detail in chapter 4.3.4. After the reduction of all the inevitable system losses, the model can now convert the available power into hydrogen. This is done with the efficiency curve explained in chapter 4.3. However, the selected strategy significantly influences the eventual conversion from power to hydrogen. The different strategies and how they work are explained in chapter 4.4. At this point, the system knows from the system block 'H_2 production', how much and when hydrogen is produced. Hence, the number of switching times, power fluctuation and operating hours can be determined. The operational hours define the amount of operational degradation, which influences the operational efficiency of the electrolyser.
Finally, in section 4.5, the possibilities of dimensioning the electrolyser are discussed. It is possible to modify the number of modules with the same total electrolyser capacity size. But it is also possible to under- or over-size this capacity by removing or adding an additional module.

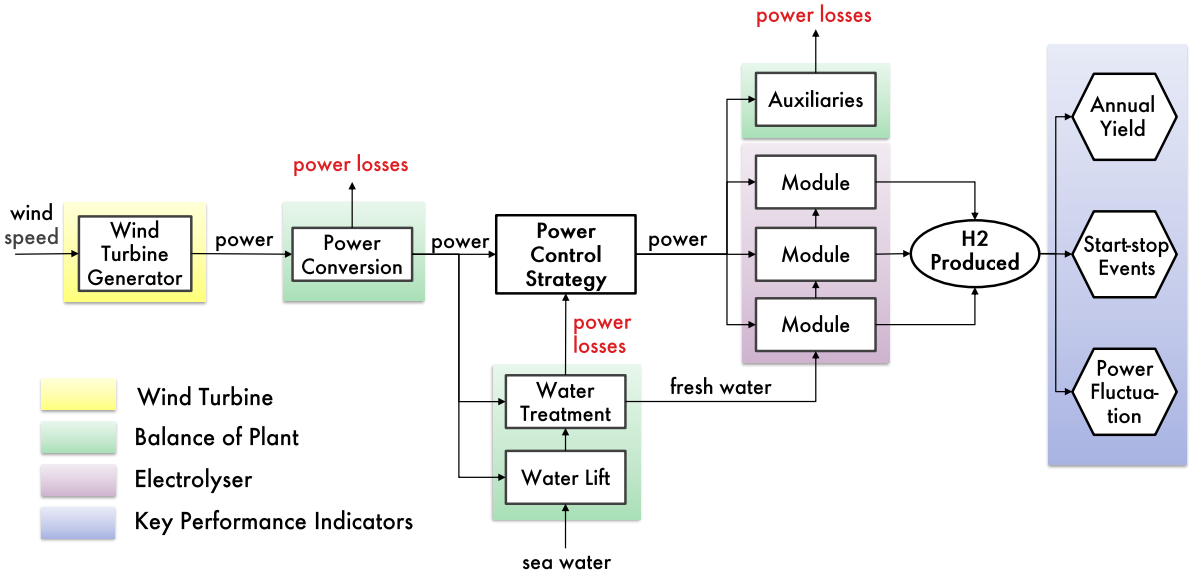

Figure 4.1: Block diagram of the system model.

4.1.2. Key Performance Indicators

Key Performance Indicators are measures that assess the success of the objective. Each KPI is individually selected with the aim of achieving the lowest LCoH. Consequently, for each KPI it is determined what metrics would best measure that aim. With fixed KPI's design objectives of the system stay clear. Since the KPI's are equally important, it is a fair method of comparing different strategies and configurations. The three KPI's used in this research are:

- Annual hydrogen yield
- Number of switching times
- Power fluctuation in the modules

The outcomes of the KPI's are determined by the input values of the model. However, because the same outcome is measured, all possible combinations of strategies and configurations can be compared on performance. The annual hydrogen yield is simply expressed as the total hydrogen production of one year in tonnes of hydrogen. For this KPI, a higher yield means an improvement. The number of switching times is expressed in the accumulation of the number of times a module switches on, in short, a start-stop sequence. For this KPI, fewer switching is an improvement. Lastly, the power fluctuation is the ramping rate experienced within a module. However, it primarily focuses on the number of fluctuations. Similarly, less number of power fluctuations are preferred. The goal of the last two KPI's is to track the potential performance degradation of an electrolyser module. Fewer start-stop sequences and fewer power fluctuations result in the extended longevity of the electrolyser modules.
It is expected that these KPI's have a trade-off with each other. For example, if the goal is to achieve the highest possible yield, this will affect the number of start-stop events and/or the number of power fluctuations. Likewise, reducing the number of start-stop events could result in a lower annual yield.

4.2. Wind input data and wind turbine modelling

The data used in this chapter is generated from a LiDAR or MET mast located on the North Sea. This data is provided by Shell. The data sheet contains information about the wind resources from 01 January 1999 until 31 December 2020 in hourly time steps. The sensors measured wind speed, wind direction and temperature at 150 meters from mean sea level. The hub height of the 15 MW IEA reference wind turbine is at 150 meters, therefore no transformation using the Wind Profile Law relation is needed.

Wind turbine modelling

To extract electricity from wind power, a wind turbine is used. The wind turbine is characterised by its power curve. The shape of this curve is similar to most other wind turbines. The model is created in such a way that it is possible to change to other turbines. However, this is outside of the scope of this study. The power curve shown in figure 3.2, is derived from equation 4.1 shown below.

$$P_w(t) = \begin{cases} 0, & v_{wind} < v_{cut-in} \\ P_{formula}(v), & v_{cut-in} \leq v_{wind} < v_{rated} \\ P_{rated}, & v_{rated} \leq v_{wind} < v_{cut-out} \\ 0, & v_{cut-out} \leq v_{wind} \end{cases} \tag{4.1}$$

$$P_{formula}(v) = \frac{1}{2}\rho C_p A v^3 \tag{4.2}$$

From equation 4.1 it is possible to calculate the power output of the wind turbine (P_w) with the use of wind speeds as an input. In this formula, v_{wind} is the actual wind speed in that hour. The operational boundaries of the wind turbine, the cut-in wind speed and the cut-out wind speed are used from table 3.3. Within these boundaries, P_{rated} is the rated power of 15 MW and $P_{formula}$ is the wind power calculation, which is described in more detail in equation 4.2.
In normal conditions the power coefficient (C_p) is a variable value, however, for simplification, a fixed value is selected. For this model, the fixed design value of $C_p = 0.489$ is used (NREL, 2020). Furthermore, a fixed air density of $\rho = 1.225\ kg/m^3$ is selected. This value is based on the geo potential altitude above sea level of 0 meter and a temperature of 15°. In reality, this is a fluctuating number and will be below 1.255 kg/m^3.
For the year 2020, the turbine operates 4023 hours at rated power, which is around 46% of the time. This year accumulates to a total power yield of 87 GW and achieves a high capacity factor of $C_f = 0.66$ directly after the generator. With this power, the electrolyser and the balance of plant can start operating.

4.3. Electrolyser modelling

This section describes how different parts of the electrolyser system are modelled. It starts with defining the efficiency curve, followed by how degradation influences the efficiency curve. Furthermore, the operation modes of an electrolyser are considered. Finally, the balance of plant modelling is explained in more detail. The chapter ends with an overview of all parameters and assumptions used in the model.

4.3.1. Efficiency curve of PEM

To simplify the modelling of a rather complex system, like a PEM electrolyser, an efficiency curve is used in this study. The efficiency curve of an alkaline and PEM systems have the same characteristic shape. The curve will be different for other kinds of electrolysers. In addition, within the same electrolysis process, the outcome of the curve is influenced by the manufacturer, size and configuration of the balance of system. Figure 4.2 shows the data points of an operational year of a power-to-gas plant with a 6 MW PEM electrolyser (Siemens Energy Silyzer 200, the predecessor of Silyzer 300 (Siemens-Energy, 2020)) in Energiepark Mainz, Germany. The data points create two lines, where the black line shows the hydrogen production as a function of the total power consumption and the green line the efficiency as a function of the total power consumption. The green line contains the typical

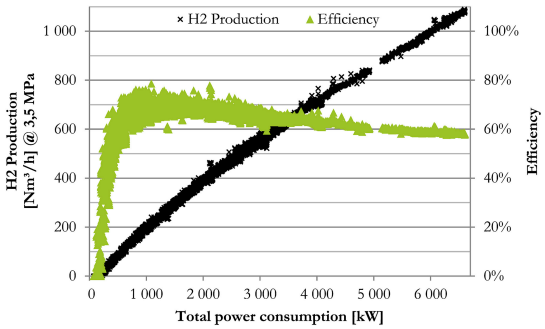

Figure 4.2: Hydrogen production and efficiency as a function of the total power consumption of 6MW PEM production plant (Energiepark Mainz) in 2015 (Kopp et al., 2017).

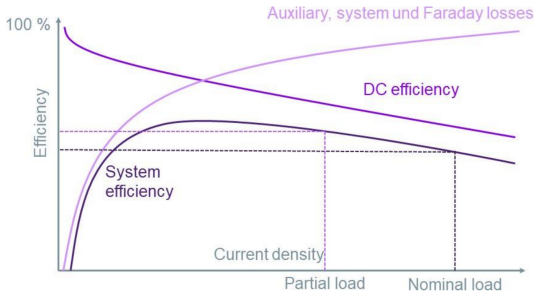

Figure 4.3: System efficiency and its schematic shape over the partial load. The system efficiency curve is determined by the shape of the DC efficiency and auxiliary, system and Faraday losses curves (Siemens-Energy & Lettenmeier, 2021).

characteristic shape of the efficiency curve of a PEM electrolyser. The shape of this curve is explained in figure 4.3. The system efficiency curve is based on the DC efficiency curve and a curve formed by the combination of auxiliary, system and Faraday losses.
The first influential curve is the DC efficiency curve, which indicates the efficiency of the stack or the module. The DC efficiency goes down when the partial load increases. The second line consists of multiple elements which each brings additional losses. These elements have in common that they have fewer losses with a higher load (e.g. pumps, rectifiers and transformers). It also contains the Faraday efficiency which describes the ratio between the actual produced and the theoretical maximum production volume. Accordingly, it accounts for diffusion losses through the membrane, electrical current losses and hydrogen losses through conversion of oxygen contamination (in the purification process) (Siemens-Energy & Lettenmeier, 2021).
Finally, the typical system efficiency curve is the result of these two lines. Depending on the supplier the curve may represent the stack efficiency, the losses of AC/DC conversion and transformation from medium voltage (power conversion), water treatment, the cooling systems and/or compression and hydrogen purification (Siemens-Energy & Lettenmeier, 2021).

The characteristic shape of the efficiency curve is higher for lower input loads, peaking at about 30% input load, followed by a constant decrease in the efficiency for higher input loads. The curve is recreated for the model and can be shaped by different design parameters. This will be discussed in more detail in the next paragraph.

To summarise, the characteristic system efficiency curve of PEM is determined by the stack efficiency and the combination of auxiliary, system and Faraday losses. This curve represents the module efficiency, the losses of AC/DC conversion (rectifier), losses of internal pumps and hydrogen purification (deoxo and drier). The shape of this curve is typically the same, but it can vary for different configurations and different manufacturers. However, the curve is independent of the electrolyser module size.

To keep the model generally usable, the typical shape of the curve is recreated and shown in figure 4.4. The curve is created in such a way that the most important parameters of this curve still can be designed. Figure 4.4, is the standard configuration based on literature. From this foundation, different input values like the minimal power load of the electrolyser, maximum power load and the peak efficiency can be adjusted. The minimal power load is where the PEM system starts operating and is visualised by the steep inclining line starting from 0%. The maximum power load is where the slowly declining line ends. The last design variable is the peak efficiency, this determines at which value the curve has the peak.
The x-axis of figure 4.4 is the partial load received by the electrolyser. So, for example, if the capacity of the module is 5 MW and it receives 2.5 MW of power (50% partial load), the operating system efficiency is about 75% (on the y-axis). For every time step, the system's efficiency is calculated. To run the system optimally, it is preferred to stay close to the peak. Consequently, to operate the electrolysers as efficiently as possible, the partial load should be within the 15-35% range. Note that if the minimal load criteria is modified and increased, the peak of the curve moves to the right.

The design parameters used for this model are based on multiple literature sources and Shell's in-house information. The selected design parameters are therefore:

- Minimum required load is set at 20%
- Maximum load is set at 100%
- Peak efficiency is set at 80%

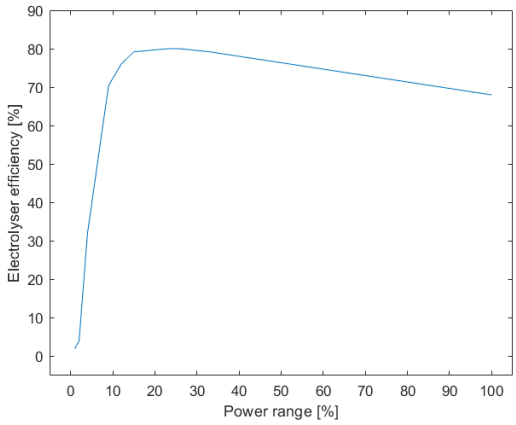

Figure 4.4: General efficiency curve for the PEM electrolyser. With minimal load criteria at 0%, maximal load criteria at 100% and peak efficiency at 80%.

Consequently, the steep line starts at 20%, has a peak efficiency of 80% at 43-46% and ends at 100% rated power.

With the efficiency curve created, the energy needed for one kg of H_2 can be determined. For this calculation, the higher heating value (HHV) of hydrogen is used, $HHV_{hydrogen} = 39.4\,kWh/kg$ (Turner, 2004). Knowing the HHV of hydrogen and the system efficiency of the module, the electrical energy used to produce 1 kg of hydrogen can be calculated with equation 4.3.

$$E_{used} = \frac{HHV_{hydrogen}}{\eta_{module}} \tag{4.3}$$

4.3.2. Degradation of the cell efficiency

Degradation issues are an important topic for water electrolysis. There are many factors that influence the degradation of the cells. However, many studies are still being conducted to understand and identify which factors contribute the most to degradation.

The effect of the efficiency degradation by operating hours is calculated using the following equation.

$$\eta_{module}(t+1) = \eta_{module}(t) * (1 - (\frac{\eta_{degradation}}{8000}) * B(t)) \tag{4.4}$$

In formula 4.4, η_{module} is the efficiency of the electrolyser module depending on hour t. $\eta_{degradation}$ is the total degradation loss of performance over 8000 operational hours and is derived from Shell (2022). This design parameter is put on 1.5%, but is adjustable. $B(t)$ indicates the state of the module, on or off.

4.3.3. Operational modes of the electrolyser

When an electrolyser is turned on or off, it goes through a cycle of different modes. The modes used in this study are full stop, cold standby, hot standby and operational.
When in a full stop, the module is cooled down to ambient temperature, the system pressure has been released and the system is inerted with nitrogen (purged). If the electrolyser is going to produce

hydrogen from a full stop, it goes from a full stop to a cold standby to hot standby before entering full operation. This complete process takes 1 hour and is accounted for in the model.
If the electrolyser is in cold standby, the module is cooled down to ambient temperature, the system pressure has dropped below operational pressure and there is minimal electrical self-consumption. The system needs to heat the electrolyser from cold standby to a hot standby before it is operational. This takes up to several minutes.
The last standby mode is the hot standby. Here the system is kept pressurised but the temperature drops slowly due to heat losses. However, it is capable to start operating in seconds, because of the better temperature. Again there is minimal electrical self-consumption.
Immediately after the hot start, the electrolyser is able to be operational. The system produces hydrogen from the minimal required load until the nominal load. The electrolyser is able to produce hydrogen in between these boundaries, which is the partial load. The ramping rate of the electrolyser depends on many factors, but for the Siemens Silyzer 300, they mention 10%/s (Siemens-Energy, 2020).
However, these modes and ramping rates take seconds to minutes. With the model working on hourly data, the details of the ramping rate and the required time from the cold and hot standby to operational are disregarded. Hence, to compensate for the loss of detail in the switching cycle, the complete cycle from a full stop to a load in the operational range is rounded up to one hour. So, if the system is in full stop mode and in the next time step there is a load, then no hydrogen is produced. If power is available for the module in the next time step, the electrolyser actually starts producing hydrogen.
This cycle is also applicable the other way around when the electrolyser is turning off. If there is insufficient power after production, then the system stays on standby for one hour. If power is available in the next time step, the electrolyser module can immediately start operating again. However, if there was no power available in the previous time step, the system would go into a full stop. Thus, if the power suddenly drops to below minimum load, but goes back into the direct next time step, then the system remains operational. If the power drops below the minimum load for longer than one time step, then for the electrolyser to start operating, it first needs to go through all modes. Therefore, one hour of power is unexploited.

4.3.4. Balance of Plant modelling

Between the produced power from the wind turbine and actual hydrogen production in the electrolyser, there are many inevitable losses of the balance of plant. First, the available power needs to be converted to the right frequency and the right type of current (AC or DC). After that, the losses of auxiliaries, water pump and water treatment are deducted. Finally, the leftover available power is used by the electrolyser under a selected strategy.
After the power production by the wind turbine, 0.1% of general operating losses of the wind turbine are accounted for. The power conversion losses are calculated with a static efficiency over the partial load range and vary per converter type. For the power conversion, it is assumed that the rectifier operates on a constant efficiency of 97%. Moreover, it is assumed that the transformer within the system operates at a constant efficiency of 98%. However, they are both a design parameter and can be adjusted for the model. To make the system more detailed, an active efficiency per partial load could be implemented. Nevertheless, this is not done to keep the model more convenient.

The model calculates how much hydrogen can be produced from the available power. However, the electrolyser needs purified water to produce hydrogen. This process consumes energy and increases the losses. As a result, the amount of available power for hydrogen production is decreased. This loop is visualised in figure 4.1. To exit this loop, the model runs two calculations in every iteration and compares the difference between the two. The first calculation predicts the water use and the losses of the water purification process with the available power. The second calculates the new amount of water use and the losses of the water purification process with the new losses included. This loop keeps on iterating and converging until there is less than 0.5% difference between the two values and is done for all electrolyser modules. Afterwards, the script continues with the actual amount of water needed combined with its losses.

The electric energy consumption ($E_{pump}(t)$) of the water lift pump is described in equation 4.5. $Q(t)$ is the volumetric flow rate of the pump. H is the height from sea level until the platform, where the pump is housed. g is the gravitational constant. ρ is the density of (North) seawater and η_{pump} is the constant

efficiency of 92%.

$$E_{pump}(t) = \frac{Q(t) * H * g * \rho}{\eta_{pump}} \tag{4.5}$$

To implement the total energy use of reverse osmosis in the model, the volumetric flow rate of seawater and the energy consumption of the desalination unit are needed. The volumetric flow rate of seawater, $\dot{V}_{H_2O}(t)$ in $\frac{m^3}{h}$, is calculated using 4.6 (Singlitico et al., 2021).

$$\dot{V}_{H_2O}(t) = \dot{m_{H_2}}(t) * W_{des} * 10^{-3} \tag{4.6}$$

W_{des} is the seawater consumption (L) for each kilogram of hydrogen produced. However, from electrolyser manufacturers, only the conversion from freshwater to hydrogen is known. In this study, it is assumed to be 10 litres of fresh water per kilogram of hydrogen. This then needs to be converted to litres of seawater. From Shell (2022), the conversion rates are known and are used in the model. However, due to confidentiality, they are not mentioned in this report. The volumetric flow rate of the desalination units is used as a value for the electric energy consumption of the desalination unit and is calculated using equation 4.7. Here e_{des} is the energy consumption per cubic meter of water processed, assumed to be 3.5 $\frac{kWh}{m^3}$ (Singlitico et al., 2021).

$$E_{des}(t) = \dot{V}_{H_2O}(t) * e_{des} * 10^{-6} \tag{4.7}$$

A part of the electrolyser losses is converted into heat. This excess heat needs to be extracted to keep the electrolyser running at an optimal temperature, hence the use of a cooling system. For this cooling system, the power needed is assumed to be 10% of the heating losses created by the electrolyser. The remaining head is dissipated by the ambient temperature.

4.3.5. Overview of parameters and assumptions for the system model

The following table gives an overview of all key parameters and assumptions of each component used.

Parameter	Value
Electrolyser system	PEM
Electrolyser capacity	15 MW
Electrolyser minimal load	20%
Electrolyser maximum load	100%
Higher Heating Value of hydrogen	39.4 kWh/kg
Operational degradation electrolyser	1.5%/8000h
Platform height	15 m
Rectifier efficiency	97%
Transformer efficiency	98%
Pump efficiency	92%
Desalination system	Reverse Osmosis
Reverse Osmosis energy consumption	3.5 kWh/m^3

Table 4.1: Overview of components with key parameters or assumptions used.

4.4. Power Management Strategy

When a PEM electrolyser is directly coupled to a single offshore wind turbine, it needs to coop with the fluctuation of the intermittent wind power. Next to the fluctuations, the electrolyser is exposed to periods of no power. This happens during periods of no, low and extreme wind speeds. The optimal goal of the control strategy is to maximise the yield, have as low as possible switching times and to reduce the amount of power fluctuation within a module. However, these goals (and KPI's) have a trade-off with each other. It is expected that when the yield is maximised, the system will encounter more fluctuation and/or more start-stop sequences. This also counts for the other way around. Yield is expressed in total annual hydrogen production. Switching times define the number of times a module is switched on. Power fluctuation can be identified by the number of power oscillations within a module.

In the industry, an electrolyser is operated at a constant power level, mostly at rated power. Consequently, there is a lack of literature about controlling an electrolyser with fluctuating power supply. In this study, three ways of power management strategies are tested. However, due to confidentiality reasons, the third strategy is not covered in this part of the report.
The strategies described in this chapter are the segmented start and the equal power division. Each strategy has its own purpose with regard to the KPI's. The goal of equal power division is to achieve the highest yield and the segmented start aims for a more balanced trade-off between the KPI's. The confidential strategy aims to extend the electrolyser's longevity by reducing the number of start-stop events and the number of fluctuations. The expectations of each strategy are summarised in table 4.2. The strategies fundamentally differ from each other by how the power is managed to each individual module. Furthermore, each strategy can be adjusted with a setpoint. The set point can be compared to a minimal powering threshold of a module and can range from 0-100%. The strategies and the effect of different setpoints are discussed in more detail below.

	Hydrogen production	**Start-stop events**	**Power fluctuation**
Segmented start	+	+	–
Equal power division	++	–	– –
Confidential strategy	–	++	+

Table 4.2: Expectations on KPI's for each power management strategy.

4.4.1. Segmented start

The first treated strategy is called "segmented start". With segmented start, the modules are started separately and switched on when a selected threshold is reached. In the first example, the modules will only run when 100% of its capacity is available. This is called the 'simple start-stop' strategy, where the threshold (setpoint) is 100%. Due to the fluctuating nature of wind power and no room within a module to fluctuate, this strategy results in a low yield and a high number of start-stop events. Therefore, running the electrolyser with this strategy will not bring any advantages. This 'simple start-stop strategy' is from Fang and Liang (2019) and is the foundation for the segmented start strategy. Despite the not so useful 'simple start-stop' strategy with a setpoint of 100%, lower setpoints can create a higher yield and fewer switching times.
To give a more detailed example, we put the setpoint at 50% with 7 MW of available power for a 3x 5 MW configuration. This example is visualised in figure 4.5. For the first step, the controller first tests how many modules can be operated at the minimal setpoint and 'fills' them with the available power to the minimal setpoint. In this example, the first two modules are now filled to 2.5 MW (50% of the module's capacity). These (partially) filled modules are called active modules. In the second step, the model checks if the active modules can be filled to rated power and does so if this condition holds. In this example, this does not happen, because there is not enough power available. For the third step, the model flags the next active module in line, which is not fully filled nor off. This flagged module is filled with the leftover power. By doing so, the leftover power will never power a module under the setpoint nor powers a module above rated power. Hence, only one module handles the fluctuating power supply per time step. In the accompanying example, the first modules will be filled with the left over power of 2 MW.

At high setpoints, the strategy is not working optimally. This is best explained with the following example. Let's say that the power available is 7.5 MW and there are 3x 5 MW modules available and the setpoint is 80%. Then, there is enough power to fill the first module with 4 MW (80% of 5MW). However, the rest of the modules are not powered. Despite, the system being left with 3.5 MW of available power, this does not trigger a new module as it is below the selected setpoint. So, the model then powers the first stack to rated power and the leftover is discarded. This is an unprecedented event, but cannot be avoided. A final example of a special situation is when setpoint is put at 0%. In this case, the model first powers the modules at rated power if applicable and finally powers the first non-active module with the left-over power. However, each module has a minimum required load. So when the power below the minimum required load is distributed to the module, it will be discarded. This results in less utilisation of the available power, hence lower yield and more start-stop sequences.

The current segmented start strategy is based on a first on, last off principle. Therefore, the modules are powered in the same starting sequence every time. In theory, it would be better to switch, which module will be powered first. Accordingly, the number of switching times are divided more equally over the modules. This will be discussed later on in chapter 7.

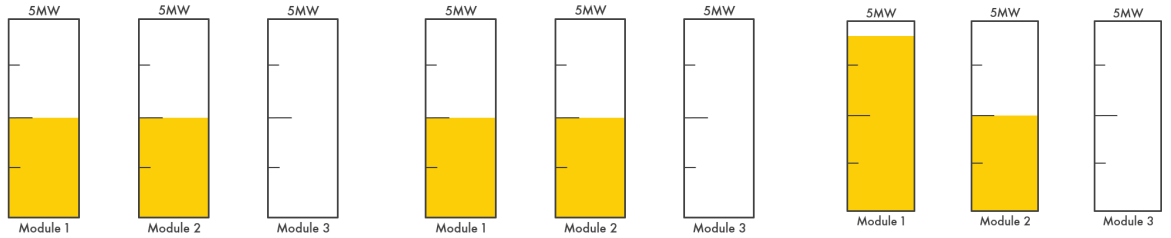

(a) First step of the segmented start strategy.

(b) Second step of the segmented start strategy.

(c) Third step of the segmented start strategy.

Figure 4.5: Simplified visualisation on how the segmented start strategy works with the example of 7 MW available power and 50% setpoint.

4.4.2. Equal power division

The second way of power allocation is an equal power distribution over the modules. This strategy powers the modules (if active) with the same amount of power. Therefore, the modules run on a higher efficiency and reach a higher overall yield. However, this also means that each module makes more operational hours and therefore suffers from higher degradation. Despite, the more degradation from the running hours, it could be a better strategy because the electrolysers are operated less on or near rated power. This also influences performance, but this is still an unexplored topic in literature. On the other hand, the modules are powered with variable loads all the time, which also could have an impact on the performance. Because of the uncertainties and hard to quantify parameters, this is not taken into account, but should be explored in future studies.

Likewise, this strategy uses a minimal setpoint. If the setpoint is put on 0%, the minimal setpoint is put aside and all modules will be active with the same amount of power. Here the same problem occurs when modules are powered below the minimum power requirement. Beneath this point, the power is curtailed, which results in a lower yield.

Using a setpoint works the same as with the segmented start strategy, however, results in different effects. How the strategy works can be best explained by an example. For this example, a setpoint of 50%, 3x 5 MW module configuration and 7 MW of available power is used. This example is visualised in figure 4.6. For the first step, the model determines the number of modules that can run on the minimal setpoint. Afterwards, these modules are filled to the used setpoint. In this example, the first two modules are filled to 2.5 MW. The second step is to divide the leftover power equally over the active modules. For this example, 2 MW is equally divided over the first two active modules. Resulting in 3.5 MW, 3.5 MW and 0 MW of power distributed over the modules .

However, similar to the segmented start, with a too high setpoint the strategy is not working optimally. This is explained in the previous section with an example. However, this has a major impact on the equal power division strategy's yield, therefore a new part in the code gets activated to prevent this from happening. This new part overrules the setpoint and redistributes the power equally over the active and the first inactive module. This additional part of the code and the difference is explained in more detail in appendix D.

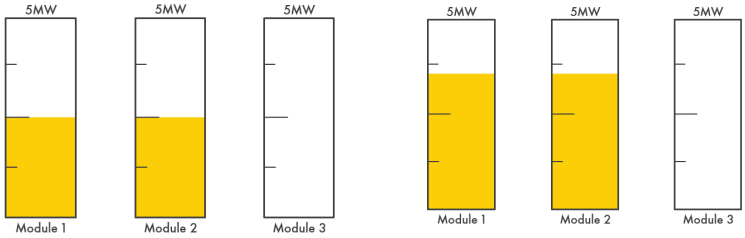

(a) First step of the equal power division strategy.

(b) Second step of the equal power division strategy.

Figure 4.6: Simplified visualisation on how the equal power division strategy works with the example of 7 MW available power and 50% setpoint.

4.4.3. Confidential strategy

The third strategy is confidential and is described in a confidential appendix (Appendix A).

4.5. Configurations of module dimensioning

It is possible to divide the 15 MW electrolyser capacity over multiple modules. As a base case, the three times 5 MW module configuration is used. This is still a novel commercial size, but is expected to enter the market soon. The current maximal market size is 2.5 MW, therefore another configuration is six times 2.5 MW. A final option that is considered is the use of one big module of 15 MW. Again, this is a novel size for a module, but could be implemented in the future. The clear effect of different module sizes is visualised in the following chapter.
For each configuration of modules with the same total electrolyser capacity, the effect of different strategies is analysed. To compare the results of different configurations, the segmented start strategy is used as a base case. For this strategy, a setpoint of 50% is selected. Again the effects will be measured by different KPI's.

In addition to module dimensioning, there is also an interplay with total capacity size. It is possible in this model to modify the electrolyser capacity. Changing the electrolyser capacity, but keeping the same wind turbine size, results in over- or under-sizing. In this study, two scenarios are analysed, namely adding and deducting a module of 5 MW to the base case configuration of three times 5 MW modules. According to Mehta et al. (2022), when designing a hydrogen producing wind turbine it is an improvement to over-size the electrolyser compared to the turbine size. Because as a result, the operating efficiency is increased (Mehta et al., 2022). These scenarios are tested with the power management strategies and are analysed by the divined KPI's.

5

Results and Discussion

This chapter analyses the results of different control strategies and module dimensioning. The chapter starts with the case-study description. The next section covers the energy flow of the system. The following section examines the impact of the different power management strategies. This section is concluded with a discussion that reflects on the results of the different strategies. The next two sections discuss the effect of module dimensioning, whereas in the first section, the impacts of smaller and larger module sizes are analysed. The second section discusses the impacts of over- and under-sizing of the electrolyser capacity.

5.1. Case-study description

All case studies are performed for the same location, meaning that for each case the wind input is the same. By using the IEA 15 MW reference wind turbine, the generated power for each case is equal as well.
The different cases will be assessed on the same wind speed data from a location on the North Sea. For a fair comparison, a typical wind year is selected from the data. Therefore the provided wind speed data are analysed in detail. An overview of the average mean wind speed of the 21-year data is given in figure 5.1.
It is important to notice that a year with more extreme high/low wind events would produce less power and eventually hydrogen than another year with the same average wind speed but milder weather. Therefore, a lot of information is lost in figure 5.1. A better way of assessing the wind speed data is to analyse how much time wind spends within the operating window of the wind turbine. Hence, it is better to look at the probability density function of each year. The probability density function of the complete wind data is given in figure 5.2. This bar plot is a good example where the probability follows a Weibull curve.

Analysing the wind data further, it is challenging to determine which year enhances the performance of the system. The total amount of electricity production is calculated using the power curve with accompanying operational boundaries. The year with the highest electricity yield is the best year and the year with the least is the worst year. From this analysis, the year 2020 is a typical year and is therefore used as the base case. However, 2020 counted 366 days. The combination of the probability density function and power curve of the 15 MW wind turbine is visualised in figure 5.3. In addition, the year 2003 is the 'worst' wind year and 2005 is the best wind year available in this data set.
For these three years, some more information is summarised in table 5.1 below. The year 2003 is used as sensitivity cases in chapter 6. The year 2005 is excluded from the sensitivity analysis, because there are no major differences with a typical year in this data-set.

As mentioned in the previous chapter, there are many possibilities for the system in regard to strategy and module configurations. To keep a clear overview of what is studied, different cases are defined and described. The possibilities of various configurations and where in the report they are discussed are shown in table 5.2.

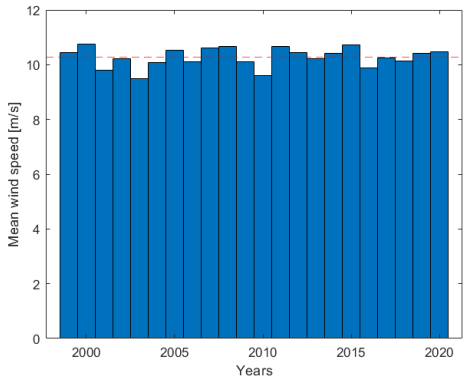

Figure 5.1: Average mean wind speed of 21 years of wind data. With a mean wind speed of 10.27 m/s.

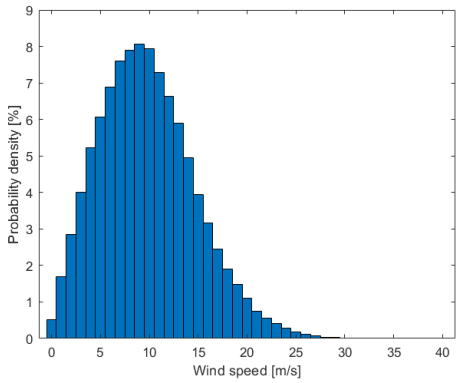

Figure 5.2: Probability density function of wind speeds over the complete data set.

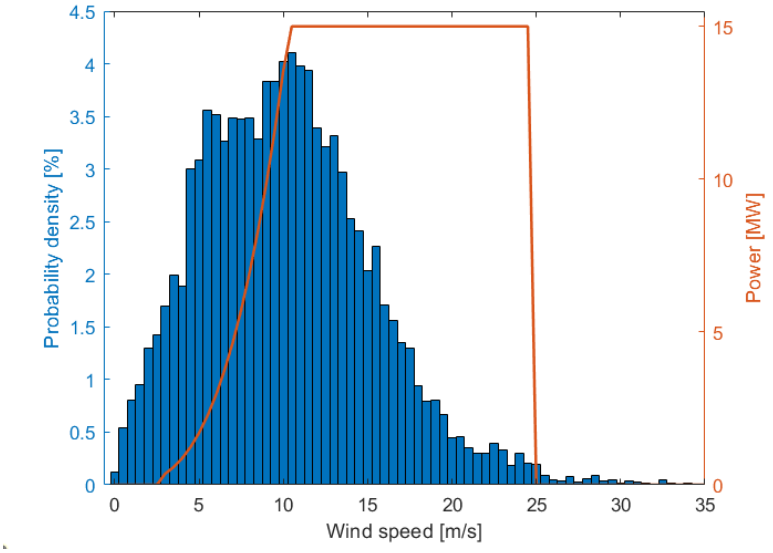

Figure 5.3: Combination of the probability density of the wind speeds throughout 2020 and the power curve of the IEA 15 MW wind turbine.

	Typical (2020)	**Worst (2003)**	**Best (2005)**
Mean wind speed [m/s]	10.47	9.48	10.52
Amount of hours wind speed below cut-in [h]	458	494	385
Amount of hours winds speed above cut-out [h]	74	9	40
Amount of hours at rated power [h]	4023	3254	4123
Longest period outside of production range [h]	23	43	19

Table 5.1: Overview of the different wind years used. The year 2020, base case, is an average year. The year 2003, is the worst wind year. The year 2005, is the best wind year.

The goal of the various cases is to bridge the generic model to specific results which can be analysed in more detail and be compared to each other. The base case is where the electrolyser capacity is equal to the wind turbine capacity, therefore it has a 1:1 ratio. The 15 MW electrolyser is divided into a 3x 5MW module configuration, correspondingly specifies the base case. The other cases are one big module of 1x 15MW and smaller modules of 6x 2.5MW. The model is capable of comparing more module sizes. However, the used cases are based on current and expected industrial module sizes. It is also possible to adjust the total electrolyser capacity, which changes the ratio. These possibilities are tested and compared as a final case study for a 2x 5 MW and a 4x 5 MW configuration.

In the case of one big 15MW module, the different power management strategies do not influence the end results. Therefore, the 1x 15MW configuration is independent of the selected strategy. Nevertheless, the strategies do influence the outcome of the other configurations, which are explained in corresponding sections.

	3x 5MW	1x 15MW	6x 2.5MW	2x 5MW	4x 5MW
Segmented Start	Ch5.3.1	Ch5.4*	Ch5.4	Ch5.5	Ch5.5
Equal power division	Ch5.3.2	Ch5.4*	Ch5.4	Ch5.5	Ch5.5
Confidential	Ch5.3.3	Ch5.4*	Ch5.4	Ch5.5	Ch5.5

Table 5.2: Overview of different cases and in which section the results of the cases are discussed.
*The strategy does not influence the outcome of the 1x 15MW configuration.

5.2. Overview of energy flow in the system

The goal of this study is to evaluate a standalone offshore wind-to-hydrogen setup. Therefore, the electricity that the turbine produces, powers all the auxiliary components of the electrolyser, also called the Balance of Plant (BoP), and the electrolyser itself. The energy flow of the system is visualised in a Sankey Diagram in figure 5.4. This figure shows the flow of energy when the wind turbine is operating at rated capacity. All unavoidable losses of different components are accounted for. Ideally, the electrolyser should get the maximum possible power from the turbine. Therefore, minimal losses are preferred.

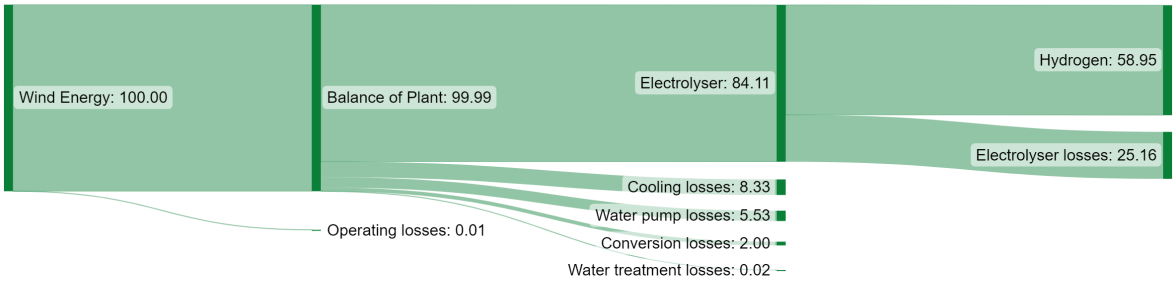

Figure 5.4: Energy flow of the system at rated power shown in percentages (%).

5.3. Impact of different strategies

This section assesses the effect on the system of different strategies. For each strategy, the effect of various setpoints is analysed. Eventually, the KPI's of the strategies are compared. First, the results of the segmented start strategy are discussed. The section starts with the results of the total annual hydrogen yield and the effect of different setpoints on yield. After that, the total switching times are analysed. Finally, the effect on power fluctuation is shown. Subsequently, the same is done for the equal power division and the confidential strategy. However, the latter is discussed in the appendix. All strategies are applied to the base case configuration, so three electrolyser modules with a 5 MW capacity.

5.3.1. Segmented start

The effect on annual hydrogen yield by changing the setpoint for the segmented start strategy can be seen in figure 5.5. The shape of the curve starts with its reduction to a minimum around the minimal load, then a gradual increase to a maximum, with a subsequent drop to a constant level at a high setpoint. The behaviour of this curve will be explained in this section.
The previously mentioned figure clearly shows that it is inefficient to operate the modules with a setpoint below 20%. As mentioned in 4.3, the electrolyser module has a minimal load threshold of 20%.

Hence, when a module is powered below this 20%, the power is curtailed. Consequently, causing a big reduction in the annual yield between 0-20%. The slope is downwards from setpoint 0% to 20% because, with each step, more power is curtailed. For example, at 0% setpoint, no power is unnecessarily wasted, while at 10% setpoint, all three modules are powered to at least 0.5 MW. In the scenario when not enough power is available to power above this number, all this power is discarded, resulting in a decrease in annual yield.
Another noticeable jump in graph 5.5 is at a setpoint above 78%. Here the annual yield keeps constant despite the increasing setpoint. This results from the combination of the available power to the electrolyser and high setpoint. Figure 5.4 shows that the maximum available power for hydrogen production is around 12 MW at rated power. To give an example with a 3x 5 MW configuration and a setpoint of 80%, the result is that the 3rd module is not powered unless a minimal power of 12 MW is available to the electrolyser. Because this does not happen, the first two modules are powered at rated power and operate with consistent efficiency. Therefore, the line is stable from this point on. Consequently, the modules are not used optimally, resulting in a decrease in annual yield. Thereby, using a setpoint above 78% is inefficient for the segmented start strategy.
The peak of the curve is at 54%, concluding that the segmented start strategy has the highest yield at this setpoint. This point is marked with a red star. At this point, an annual yield of 1224 tonnes of hydrogen is achieved.
The increase from the minimum required load until the peak can be explained by the fact that the modules are operated more and closer to the peak efficiency and less power is being curtailed.

Figure 5.6, shows the effect of the segmented start strategy on the number of switching times per module for each setpoint over one year. Together they form the total number of switching times. There are a few observations that are noticeable in the figure. First and foremost, increasing the setpoint raises the total amount of switching times. The mechanism driving this behaviour is that there is more fluctuation in power in the higher power range (7.5-15 MW), which originates from the wind data. With the setpoint as a threshold in place, this results in more start-stop events.
Secondly, the switching times of the first module are not affected by altering the setpoint. Due to the fact that the first module is always powered first, it reached the maximum amount of switching time in every setpoint for this specific year.
Thirdly, after a quick increase of switching times to a setpoint of 20%, the total number of switching times steadily increases per setpoint step onward. Until 67%, where the maximum amount of switching times is reached. The reason behind the maximum number of start-stop events is also in the nature of wind fluctuation throughout the year.
Finally, there is a particular case at the beginning where the setpoint is at 0%. At this setpoint value, there is no threshold when a module should be turned on, consequently causing many switching within the modules. This increase in switching is caused by the sensitivity towards fluctuation without a setpoint.
At the peak production setpoint of 54%, the modules experienced 661 switching times combined.

The final figure belonging to the segmented start strategy is figure 5.7. This figure contains a 1D scatter plot and a histogram, which visualises the power fluctuation within a module. Figure 5.7a is basically the top view of figure 5.7b. Each point in figure 5.7a is the change in power between two subsequent time steps in the simulation per module. When combined, they visualise the power fluctuation. The outcome of this figure relies on the selected setpoint. A pragmatic setpoint of 50% is selected to later compare the results of power fluctuation for different strategies. Figure 5.7b, shows the frequency in percentage of the total occurrences in power fluctuation within a module. Analysing the figures, one can conclude that the first module copes with to most power fluctuation, then the second and lastly the third. For the first module, the power fluctuation happens more in smaller steps. The reason for this is that the first module receives the most leftover power. It is noticeable that with a setpoint of 50% the third module mostly fluctuates with steps of 50%, 2.5MW in this scenario. This can be explained by the fact that most of the leftover power is captured by the first or the second module, so the third module is mostly just being switched on to operate at the 50% setpoint level or switched off from it. Next to that, because of all auxiliary losses, the third module is not fully utilised. Simply because there is less power available, the third module will experience smaller fluctuations, due to its high power operational range.

To put the power fluctuation in numbers, the average fluctuation and the number of changes are analysed. Accordingly, the absolute values of all data points are used. Additionally, the values that are zero (or close to zero due to degradation) are extracted. From the remaining data, the mean power fluctuation and the number of fluctuations throughout the year can be determined. The first module has an average power fluctuation of 0.82 MW and changes 4148 times throughout the year 2020. The second module has larger fluctuations with a mean value of 1.57 MW, but experienced fewer fluctuations with 1422 shifts. The third module experienced bigger fluctuations with an average of 2.4 MW. But, only 583 fluctuations took place.

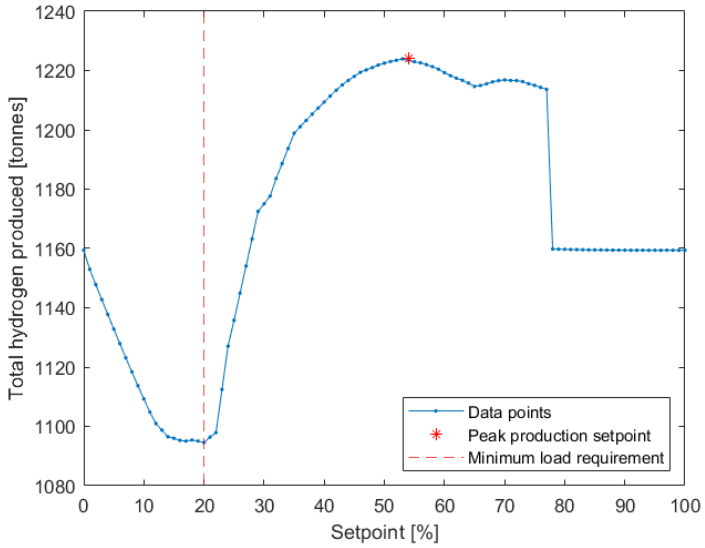

Figure 5.5: Annual yield of hydrogen for the segmented start strategy per variable setpoint. The peak of the annual yield is 1224 tonnes of hydrogen at a setpoint of 54%.

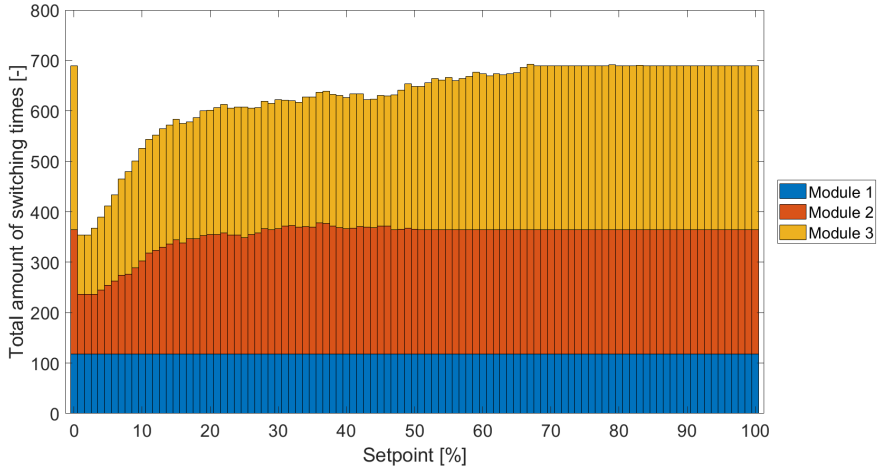

Figure 5.6: Total number of switching times for the segmented start strategy per variable setpoint.

The model calculates the electrolyser degradation over time for each module. However, only the end-of-life degradation factor is of relevance to this study. The selected setpoint influences the outcome of the end degradation. For a one-year simulation of the year 2020, using a segmented start strategy with a setpoint of 50%, the degradation in efficiency for module 1 is 98.45%, module 2 is 98.91% and module 3 is 99.04%. In this year modules operated 8257, 5823 and 5146 hours respectively.

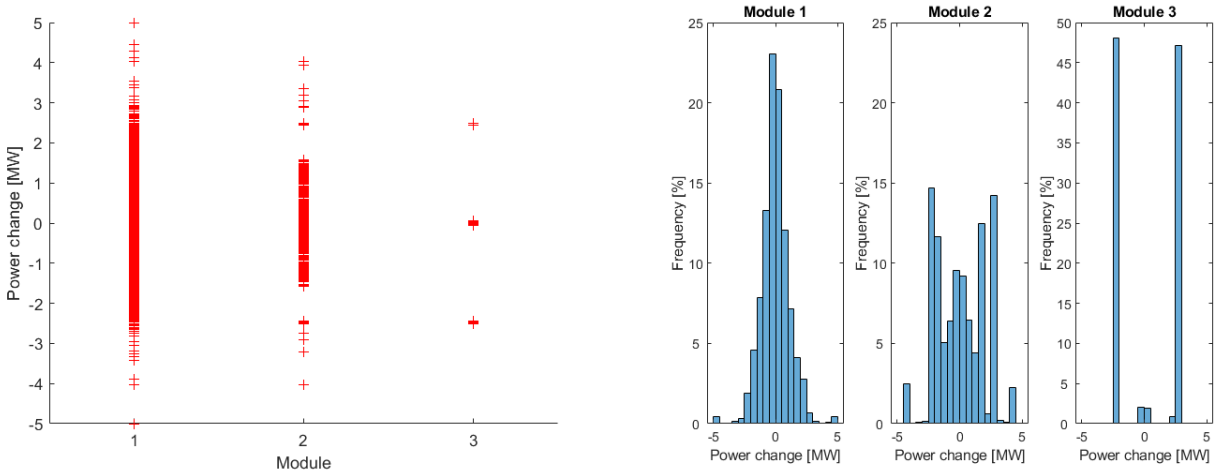

(a) 1-D scatter plot of the distribution.

(b) Histogram of the distribution.

Figure 5.7: Power fluctuation within the modules for a 3x 5MW configuration with the segmented start strategy and a setpoint of 50%.

5.3.2. Equal power division

The effect of altering the setpoint for the equal power division strategy (with the overruling code for high setpoints (explained in Appendix D)) can be seen in figure 5.8. The curve starts at its lowest annual yield and then enters a gradual increase to a maximum from where it decreases again, before going stable at a high setpoint. Again, the figure shows that operating at a low setpoint is an inefficient way. This is once again caused by the design parameter of the minimum load requirement of the electrolyser to operate. Even if the power is allocated to the electrolyser module, but is below the minimum load requirement, the power will be curtailed. Which causes the low annual yield in the starting range of the curve. The peak of the curve is at 35%, at this point the highest annual yield is achieved. The annual peak yield is 1249 tonnes of hydrogen. This is in line with the expectations for this strategy, as a higher yield can be achieved at a lower partial load in terms of the system's efficiency curve. When all available power is equally distributed, the modules run on a lower partial load and therefore at a higher efficiency. Accordingly, with this strategy, the system's power is more efficiently converted into hydrogen. A higher setpoint would cause the system to deviate from this high efficiency point.

The second figure below, figure 5.9, shows the total number of switching times for the equal power division strategy for the wind year 2020. Here, again, the switching time of the first module is not affected by the setpoint. Furthermore, at a setpoint below 20%, a lot of power is curtailed, resulting in less powering and therefore less switching of the electrolyser modules. After a setpoint of 20%, the total number of switching times steadily increases with a higher setpoint. This happens until 67%, where afterwards the total number of switching times does not change. Only at a setpoint of 100% does the total number of switching slightly increase.
At setpoint 35%, where the highest yield is achieved, the electrolyser experienced 628 start-stop events throughout the year.

The final graphs in figure 5.10 is a result of the equal power division, which shows the fluctuation within the modules at a setpoint of 50%. These figures clearly show the effect of the strategy, as a lot of fluctuation is happening in all three modules. Interesting about figure 5.10a is the gap between 1.5 and 2.5 MW in the second and the third module. This can be explained by the selected setpoint. For this strategy with a setpoint of 50%, the power range for when a module becomes active or not is predetermined. For example, the second module operates from at least higher than 2.5 MW, because at this point, the module is activated or deactivated. However, at this point, not enough power is available to power the third module. Afterwards, the module operates below 1.25 MW, where the active module can freely fluctuate. However, above this value, the third module becomes active. The same reasoning is applicable to the third module. However, if the available power becomes higher than 11.25 MW, it

is possible to see a fluctuation of more than 1.25 MW within each module. This is what causes points above the 1.25 MW range.
Looking at the mentioned figures and understanding the strategy, it is expected that the first module fluctuates a lot more with small time steps. According to the model, this is certainly the case. The first module has an average step size of 0.65 MW and fluctuates 4490 times throughout the year. For the other two modules, fewer fluctuations and bigger step sizes are expected. This is again confirmed, with for the second module a mean step size of 1.03 MW and 2197 fluctuations. Finally, a step size of 1.44 MW and 1553 fluctuations for the third module.

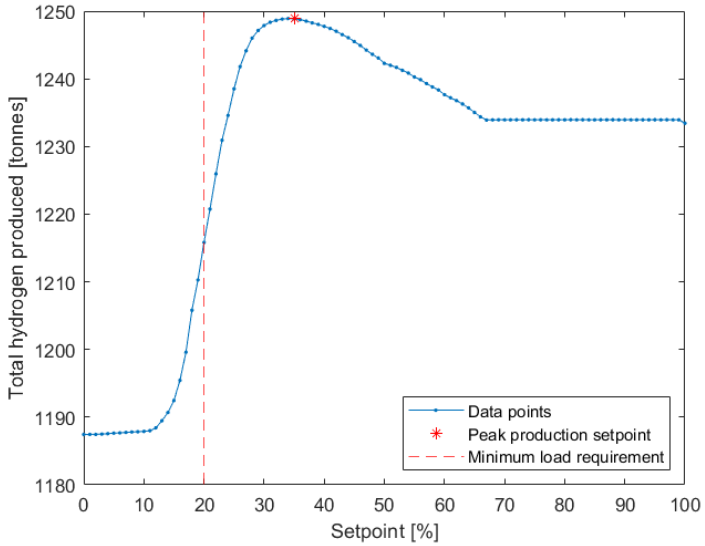

Figure 5.8: Annual yield of hydrogen for the equal power distribution strategy per variable setpoint. The peak of the annual yield is 1249 tonnes of hydrogen at a setpoint of 35%.

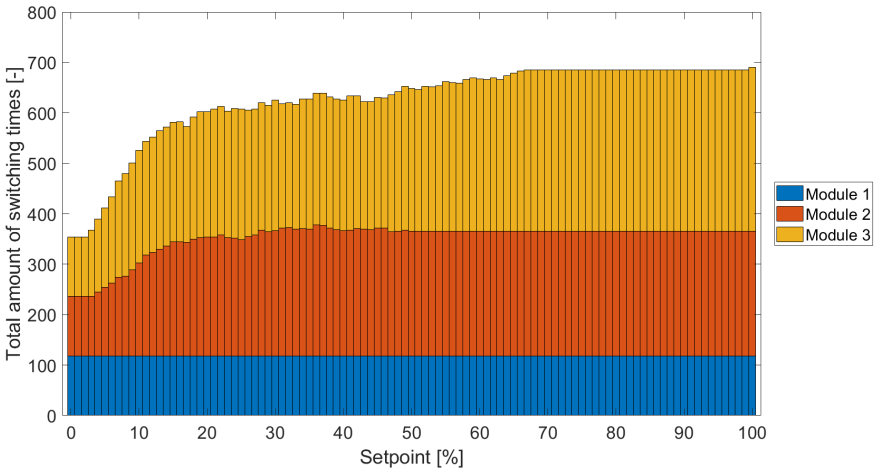

Figure 5.9: Total number of switching times for the equal power distribution strategy per variable setpoint.

For a one-year simulation of the year 2020, using the equal power division strategy with a setpoint of 50%, the cell degradation factor for module 1 is 98.45%, module 2 is 98.91% and module 3 is 99.04%. In this year modules operated 8257, 5823 and 5140 hours respectively.

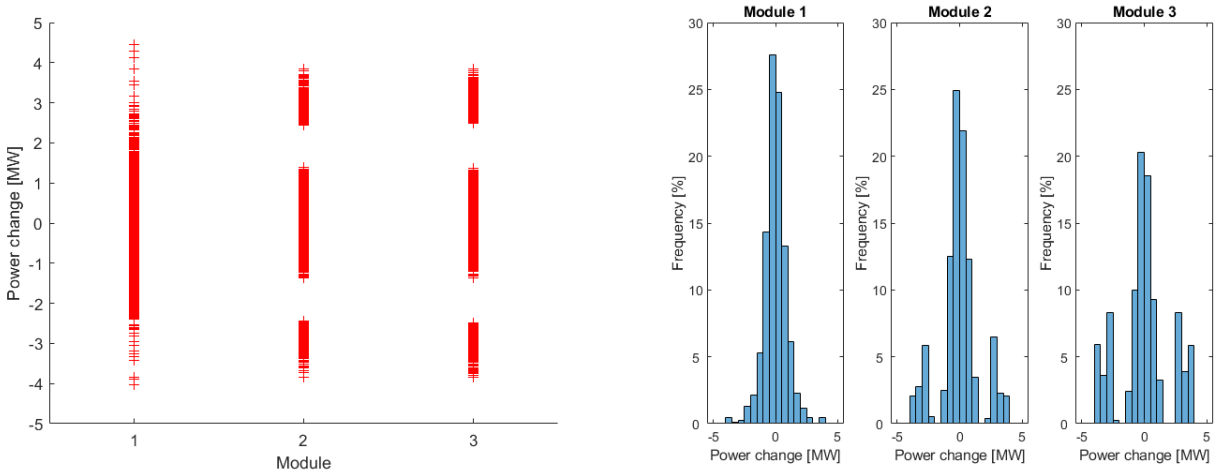

(a) 1-D scatter plot of the distribution.

(b) Histogram of the distribution.

Figure 5.10: Power fluctuation within the modules for a 3x 5MW configuration with the equal power division strategy and a setpoint of 50%.

5.3.3. Confidential strategy

The results of the third strategy are confidential and are analysed and discussed in a confidential appendix (Appendix A).

5.3.4. Discussion on different strategies

The results of the previous chapters, where the impact on KPI's by different strategies and various setpoints, are summarised in table 5.3.

	Average annual yield [tonnes H2]	Average start-stop events	Number of fluctuations
Segmented start	1173	213	6153
Equal power division	+5%	-3%	+34%
Confidential strategy	-	-	-

Table 5.3: Comparison of KPI's for different strategies.

Comparing the results of the two strategies, it is clear that the equal power division scores higher on annual hydrogen yield. This is visualised in figure 5.11. On average, over all setpoints, the equal power division strategy scores 5% higher than the segmented start strategy. This is a significant improvement solely established by a power management strategy. The increase in annual yield for this strategy results from operating the modules on a lower partial load and therefore operating the system at a higher efficiency.
In addition, the annual peak yield results can likewise be compared. For this comparison, the equal power division on a setpoint of 35% produces 2% more hydrogen over a year compared to the segmented start with a setpoint of 54%.
Figure 5.6 and figure 5.9 show quite some similarities, however they are not identical. The following graph, figure 5.12, compares the total number of switching times of the segmented (orange line) and the equal power division strategy (blue line). The main difference between the two strategies is the effect of switching times at 0% for the segmented strategy. Next to that, the equal power division achieves fewer switching times at higher setpoints. Averaged over all setpoints the equal power division achieves a reduction of almost 3% on the total number of start-stop events. In addition, comparing the peak production setpoints, the equal power division strategy experiences 5% less switching times. Not only is this the result of dividing the power more equally over the modules and therefore stretching the operational hours, but also because the setpoint used is lower.

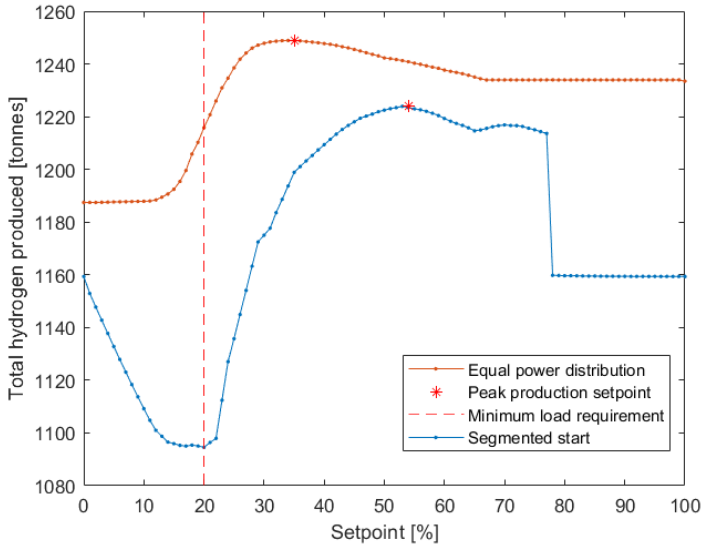

Figure 5.11: Comparison of the annual yield between the segmented start strategy and the equal power distribution strategy, per variable setpoint. The segmented start strategy is the line below, equal power division line on top.

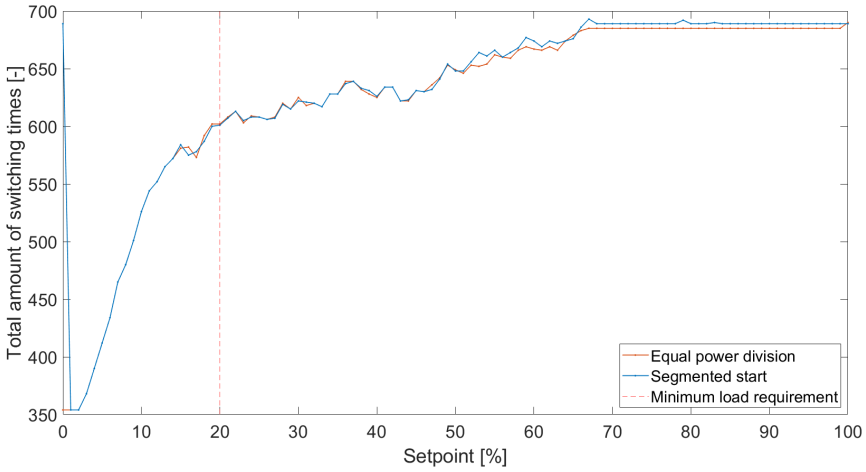

Figure 5.12: Comparison of the total number of switching times for the segmented start strategy and the equal power distribution strategy, per variable setpoint.

Reviewing the third KPI, where the power fluctuation of both strategies are analysed and compared. The sum of experienced fluctuation depends on the selected setpoint, therefore for a fair comparison between the total number of fluctuations per strategy the setpoint is fixed at 50%. It can be concluded that in general, the equal power division experiences more fluctuation of 34% more compared to the segmented start strategy. This is in line with the expectation, because the fluctuation is divided over multiple modules. Therefore, the equal power division experiences more fluctuations but with a smaller power step.

To conclude, the equal power division strategy achieves a better performance on the first two KPI's, than the segmented start strategy. The segmented start does however score better on the power fluctuation. This results in a preference for the use of the equal power division strategy.

5.4. Impact of different configurations

In this section, the segmented start and the equal power division strategies are used to compare the results of modifying the number of modules in a configuration. The analysed configurations are 1 big module of 15 MW and separating the capacity over 6 modules of 2.5 MW each. Figure 5.13 shows the difference in hydrogen production over wind speed per configuration. In this figure, the segmented start strategy is used as the base case to compare the results of different configurations. For this strategy, a setpoint of 50% is selected. However, a strategy and therefore a setpoint, are not applicable to the one big 15 MW module.
The curves are similar to the power curve of the wind turbine, but in the first part of the curve, the figures are distinguishable. Here the number of steps in the line are caused by the number of modules. So, three in figure 5.13b and six in figure 5.13c. The curves for the equal power division strategy are similar to the curves displayed below, however the segments are less visible. Because of the similarity, they are shown in Appendix B. It is clear to see that the minimum required wind speed to produce hydrogen shifts to the left while increasing the number of modules. This is caused by the minimum load requirement of a module. To compare, with the minimal load requirement of 20% of a module, a module of 5 MW requires at least 1 MW of available power to start operating. While a smaller module of 2.5 MW only requires 0.5 MW of available power to produce hydrogen. Another point to notice is that increasing the number of modules decreases hydrogen production at rated power. This can be explained by the same phenomena as before, but now the smaller modules operate at a higher partial load and therefore at a lower efficiency. The difference in the minimum required wind speed and hydrogen production at rated power is visualised in figure B.2. However, due to the close resemblance in the increasing part of the curve, this figure is chaotic and put in Appendix B. The area below the line gives more information on the expected annual yield and which configuration produces more hydrogen.

The ideal configuration for a fixed capacity does depend on the location and the accompanying wind speeds. If the selected location expects lower average wind speed, it is better to have multiple smaller modules, because of the lower operational range. While if the location expects more constant high wind speeds, then a configuration with fewer modules suits better, because a higher yield is achieved.

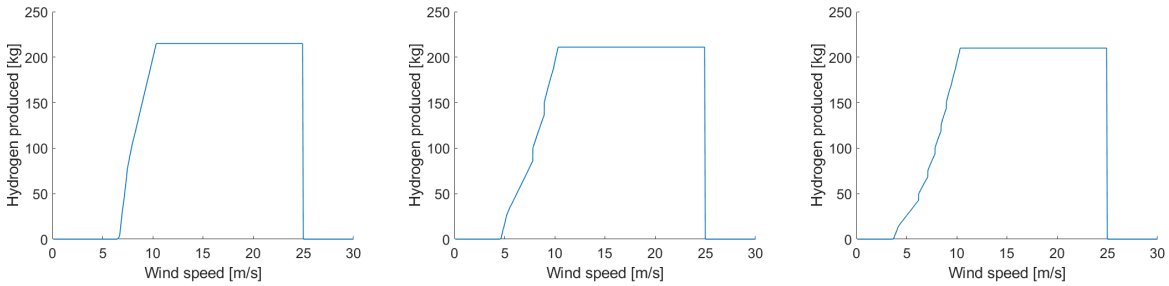

(a) 1x 15MW module configuration (b) 3x 5MW with segmented start strategy (c) 6x 2.5MW with segmented start strategy

Figure 5.13: Hydrogen production curve over different wind speeds for the three different module configurations. The segmented start was selected as a strategy for the last two figures.

Using different module configurations influences the switching times as well. The model gives the total number of switching times and hydrogen yield in a year. For the year 2020, one big module switches 118 times and achieves a yield of 1188 tonnes of hydrogen.
The two other configurations can be compared and are influenced by the different strategies and setpoints. This is shown in figure 5.14. Here, the top row shows the segmented start strategy and the bottom row the equal power division. In the left column, the annual yield per setpoint is displayed and in the right column the total number of switching times.

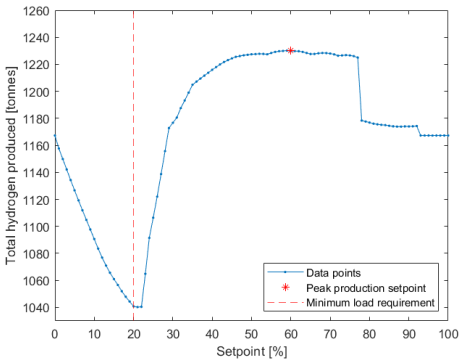

(a) Annual hydrogen yield for a 6x 2.5MW configuration with segmented start strategy.

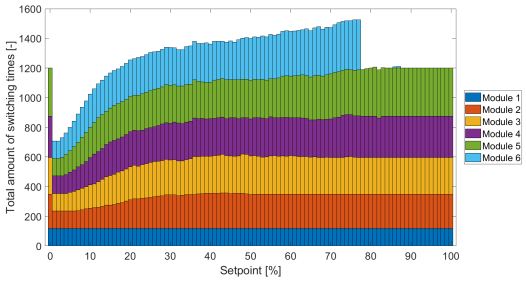

(b) Total number of switching times for a 6x 2.5MW configuration with segmented start strategy.

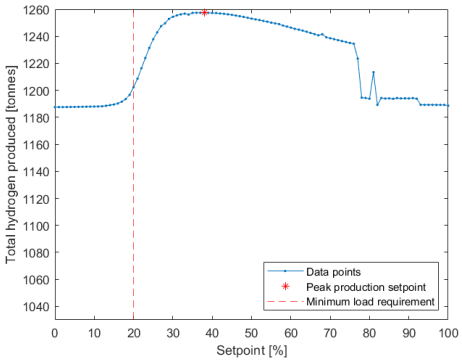

(c) Annual hydrogen yield for a 6x 2.5MW configuration with equal power division strategy.

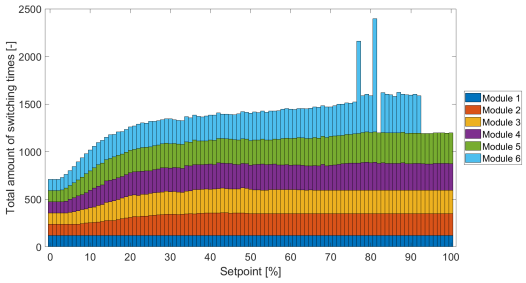

(d) Total number of switching times for a 6x 2.5MW configuration with equal power division strategy.

Figure 5.14: Graphs displaying the total annual yield and the total number of switching times for a 6x 2.5MW configuration comparing the effect of different strategies.

Comparing the effect of different configurations, depicted in figure 5.14a and 5.14c, it can be concluded that for both strategies, the annual yield is slightly increased in the optimal setpoint range and slightly decreased outside the optimal range when having smaller modules. Next to that, the setpoint where the highest annual yield is achieved, shifts to the right. For the segmented start strategy, this point moves from 54% to 60% and for the equal power division strategy from 35% to 38%. For the segmented start strategy, the change to smaller modules results in an annual yield of 1230 tonnes at the optimal setpoint of 60%. This is an increase of 0.5% and is the result of having more modules operating on a lower partial load and therefore a higher efficiency. However, at this setpoint, the total number of start-stop events and the number of fluctuations experienced has increased compared to the base case.
This same effect causes an increase of 0.6% for the equal power division. The maximum annual yield of 1257 tonnes of hydrogen is achieved at a setpoint of 38%. Likewise, the number of start-stop events and power fluctuations has increased compared to the base case.
Furthermore, it is noticeable that the segmented start strategy with more modules is more sensitive to low operating setpoints (below 20%). Here even less hydrogen yield is achieved compared to the 3x 5MW configuration. This can be explained by the fact that more power is curtailed over more modules when a low setpoint is used. This is not the case for the equal power division start. However, this strategy is more sensitive to high setpoints. After the peak value, the steadily decreasing line is extended from 67% to 78%. After the 78%, the annual yield decreases much more than for the 3x 5MW configuration. This is caused by the effect of having a too high setpoint, for the amount of power available. Therefore, underutilising the last module and effectively running the active modules on a higher partial load. Which in turn operates on a lower efficiency, causing a lower annual yield. This effect is best visible in figure 5.14b and figure 5.14d. These figures show the total number of switching times for a 6x

2.5MW configuration for the two strategies. Besides the drop at a high setpoint, the typical high peak of switching times at 0% for segmented start is again visible.
Observable in figures 5.14c and 5.14d is the spike just before 80%. They are consequences of each other because the frequent switching allows for a bit more yield. However, the cause of the spike is hard to explain. It has not been verified whether these are consequential to the model or that they are caused by the implementation in MATLAB. Nevertheless, because the spike happens at a high setpoint (non-interesting part), there is no influence on the end conclusion.
The results of using different configurations are summarised in table 5.5.

To make a fair comparison between different configurations in terms of the total number of switching times, we look at the switching at module level. The reason for this is that with more modules, the total amount of switching times increases. Looking at the mean of switching times per module, displayed in table 5.4, the equal power distribution switches more than the segmented start strategy. Because the annual hydrogen yield graphs per configuration and strategy are shown in each chapter, the figure where all these graphs are compared is put in Appendix C.

	Mod. 1	**Mod. 2**	**Mod. 3**	**Mod. 4**	**Mod. 5**	**Mod. 6**	**Total average**
Segmented start (6x 2.5MW)	118	213	231	247	267	200	**213**
Equal power division (6x 2.5MW)	118	210	229	249	264	272	**223**
Segmented start (3x 5MW)	118	234	278	-	-	-	**210**
Equal power division (3x 5MW)	118	233	273	-	-	-	**208**

Table 5.4: Mean value over setpoints of switching time per module.

		Segmented start	**Equal power division**	**Confidential strategy**
1x 15MW	**Average annual yield [tonnes H2]**	1188		
	Average start-stop events	118		
	Number of fluctuations	4491		
3x 5MW	**Average annual yield [tonnes H2]**	1173	1228	-
	Average start-stop events	213	207	-
	Number of fluctuations	6153	8240	-
6x 2.5MW	**Average annual yield [tonnes H2]**	1174	1221	-
	Average start-stop events	214	219	-
	Number of fluctuations	8854	15858	-

Table 5.5: Comparison of KPI's for different strategies with the same total capacity, but different electrolyser module configuration.

5.5. Impact of different electrolyser capacity size

This section discusses the effect of over- and under-sizing of the electrolyser capacity. The dimensioning is based on the base case of 3x 5MW modules. In the under-sizing, one module is deducted from the configuration, so 2x 5MW. For the over-sizing one module is added, 4x 5MW. Figure 5.15, shows the annual yield per setpoint, with the under-sizing in the top row and the over-sizing in the bottom row. Furthermore, the left column shows the segmented start strategy and the right column the equal power division. The second figure, 5.16, is built up similarly. Here the total amounts of switching times are compared for over- and under-sizing of the electrolyser capacity.

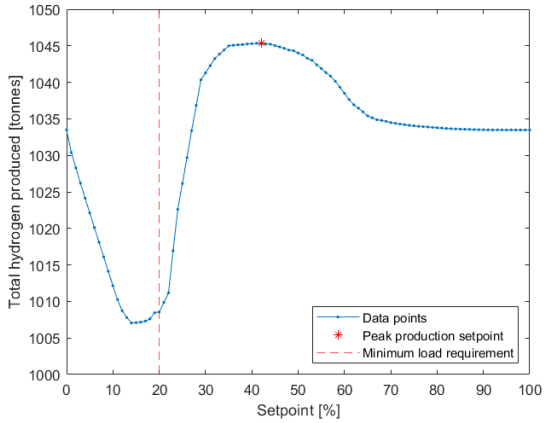

(a) 2x 5MW configuration with segmented start strategy.

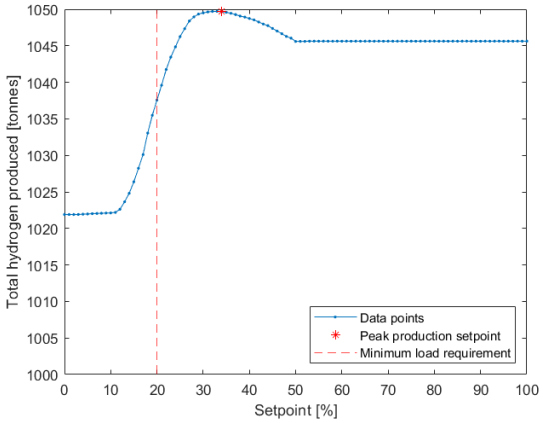

(b) 2x 5MW configuration with equal power division strategy.

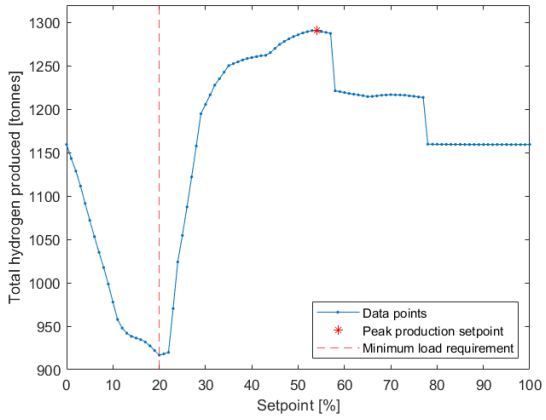

(c) 4x 5MW configuration with segmented start strategy.

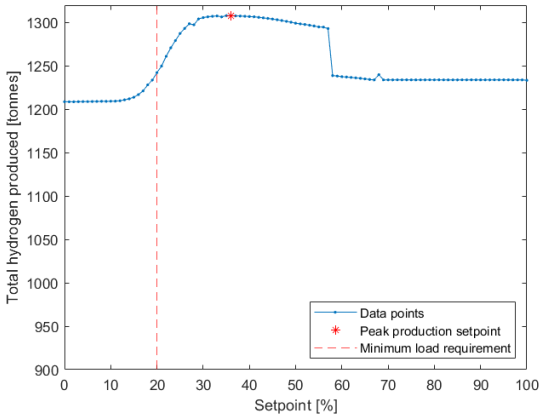

(d) 4x 5MW configuration with equal power division strategy.

Figure 5.15: The effect on annual yield per strategy for over and under sizing of the electrolyser capacity.

In the case of under-sizing the electrolyser capacity in 5.16 a and c, the annual yield moves smoother over the setpoints. Showing that in this case, the setpoint has less influence on the annual yield. Since there is less capacity available the modules operate more at a high partial load, resulting in this smoother curve. Except for the low setpoint region, where still less yield is achieved. Despite a decrease of 33.3% of capacity, the annual yield only decreases by 15% for the segmented start strategy and 16% for the equal power division compared to the base case configuration on the peak setpoints.

With 5MW of added electrolyser capacity, we see an increase of 5% at the peak setpoint for both strategies in annual yield. However, by increasing the electrolyser capacity by 33.3%, a higher overall yield is expected. This is caused by the under-utilisation of the oversized part of the electrolyser. The underutilised part comes from the fact that the wind turbine cannot produce more than rated power. In

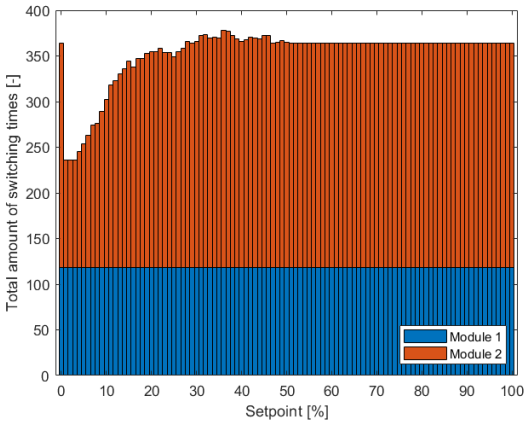

(a) 2x 5MW configuration with segmented start strategy.

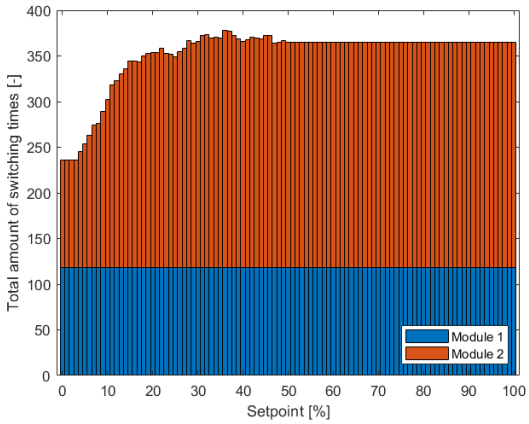

(b) 2x 5MW configuration with equal power division strategy.

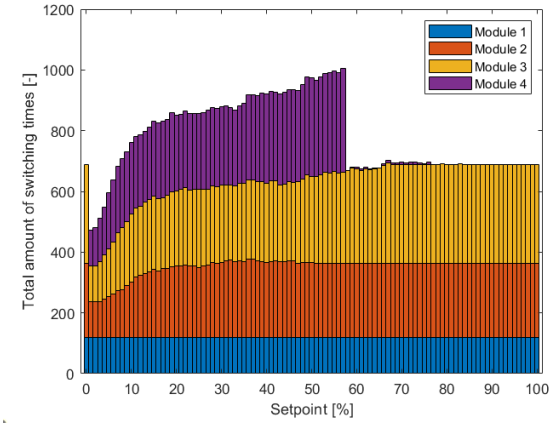

(c) 4x 5MW configuration with segmented start strategy.

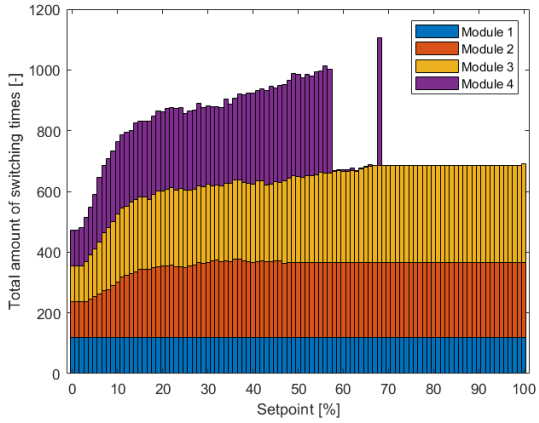

(d) 4x 5MW configuration with equal power division strategy.

Figure 5.16: The effect on the number of switching times per strategy for over and under sizing of the electrolyser capacity.

addition, the auxiliary system consumes a part of the available power. So, a larger part of the electrolyser capacity is unused. In spite of this, by operating at a lower partial load, the modules run more efficiently. It is therefore not recommended to over-size the electrolyser in regards to yield. Nevertheless, over-sizing could compensate for switching and power fluctuation.
Figure 5.15a and 5.15c are combined and compared in Appendix E.

Looking at graphs from figure 5.16, and comparing this again on module level to the three times 5 MW configuration. It is noteworthy that the bar plots stay the same for the first three modules for each strategy. Please note, that figure 5.16a and 5.16b only use two modules, but are also the same for the first two modules of the base case configuration. Therefore, it can be concluded that dimensioning in the form of over and under-sizing does not influence the switching times of the individual module.

In the situation of over-sizing, the two bottom graphs in both figures 5.15 and 5.16. It can be seen that at a setpoint of about 55% the fourth module becomes underutilised. This is again the result of the maximum available power in the system and the minimal needed threshold for the fourth module. For example, with a setpoint of 55% and 4x 5MW configuration, at least 11 MW of power needs to be available. This does occur, but this does not guarantee a higher annual yield.
In figures 5.15d and 5.16d, a spike appears at a setpoint of 68%. The spikes are related to each other, because despite the increase in switching times, the modules have more operational hours and therefore slightly increase the annual yield. This however is not a desired trait, because switching the modules so frequently increases the degradation.

6

Sensitivity Case Study and Results

In this chapter, the results of modifying important design parameters are analysed. First, the input data is changed to a year with worse wind conditions than the base case. This year is selected in section 5.1. Secondly, the minimal required load of the electrolyser is altered and the results are analysed.

6.1. Different wind input case

For this sensitivity analysis, the year 2003 is used as input data and is explicitly applied to the base case configuration (3x 5 MW). As discussed in section 5.1, from the available data 2003 achieved the worst on power production for the selected wind turbine. Therefore, this year is used to show the effect on the system and its strategy. The goal is to analyse the differences with the base case and how different strategies perform under worse conditions. The expectations for operating the system in a year with less ideal wind conditions are straightforward in regard to the KPI's. Namely, the annual yield will be lower, there will be more start-stop events and fluctuations. Nevertheless, the interesting part is how will the strategies perform under other conditions. Will another strategy flourish in worse conditions?

First, the results of changing the input year to 2003 with segmented start strategy are discussed. The most interesting result is that the shape of the annual yield curve over various setpoints stays remarkably similar compared to the base case. This is visualised in figure 6.1 a&b. Therefore, the effect of a setpoint is clear to see, despite the changed input data. Even the highest yield point stays on the same position at 54%, but now with less hydrogen yield of 1107 tonnes, a decrease of almost 6%. The abrupt dip occurs again at 78%, however, the difference in yield is less. Nevertheless, the dip at the beginning of the curve is deeper and steeper compared to the base case. So, the worse wind conditions influence the outcome more in the lower setpoint region. On average across all setpoints, 2003 achieves 10% less annual yield, due to unfavourable conditions.
The total number of start-stop events also is increased in this sensitivity case. This plot is shown in figure 6.1 c&d. From this graph, the increase compared to the base case is clearly visible. Mainly, between 20% and 78% the increase takes place. After this point, the number of events stabilises at a higher number of switching times, due to an inefficient high setpoint. On average across all setpoints the start-stop events throughout the year are increased by 7%.
The operational hours are also decreased by 0%, 10% and 14%, per module respectively. Analysing the switching times at module level, on average the first module has 120, start-stop sequences, the second and third 272 and 283 respectively. This is an increase of 2%, 16% and 2%.
When comparing the power fluctuation for the same strategy but another wind input year, the results are in the same order. Visualised in figure 6.1 e&f. The first module has average fluctuations of 0.76 MW and a total of 4917 fluctuations throughout the year, the second module 1.64 MW and 1446 fluctuations, and the third module experiences on average big fluctuations of 2.35 MW, but less total number of fluctuations of 633. The fluctuation is similarly divided over the modules like in the base-case scenario, therefore the sum of fluctuations is compared. From this comparison it is determined that the system experiences 14% more fluctuations over the year.

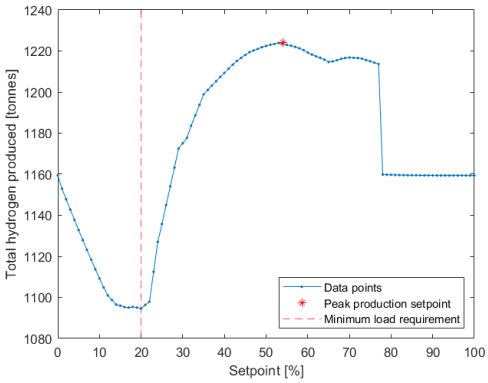

(a) Annual yield of H_2 for the segmented start strategy per variable setpoint for 2020.

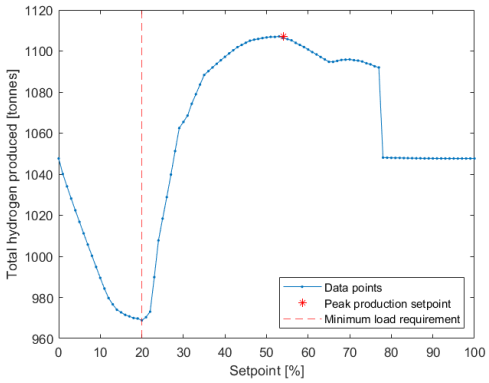

(b) Annual yield of H_2 for the segmented start strategy per variable setpoint for 2003.

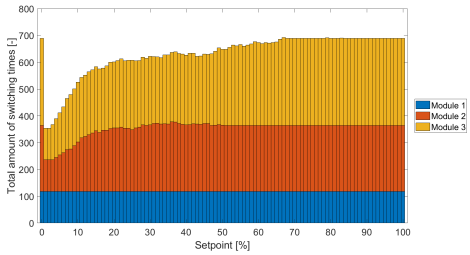

(c) Total number of switching times for the segmented start strategy per variable setpoint for 2020.

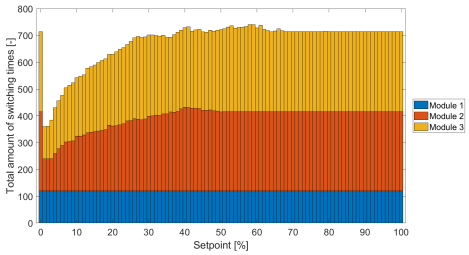

(d) Total number of switching times for the segmented start strategy per variable setpoint for 2003.

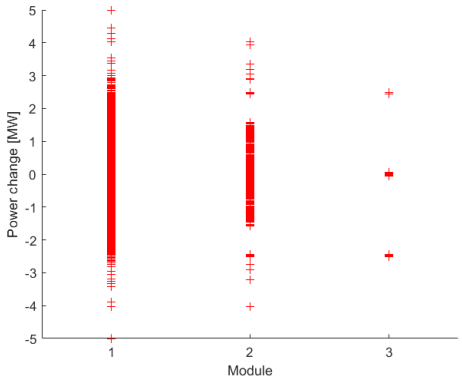

(e) Power fluctuation within the modules for a 3x 5MW configuration with the segmented start strategy and a setpoint of 50% for 2020.

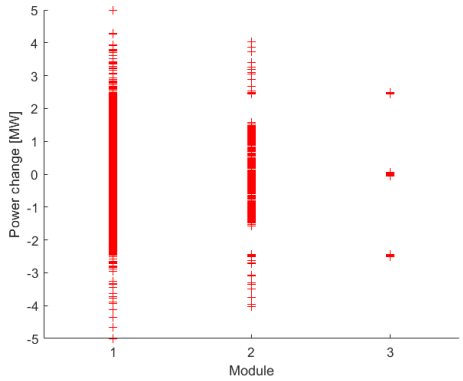

(f) Power fluctuation within the modules for a 3x 5MW configuration with the segmented start strategy and a setpoint of 50% for 2003.

Figure 6.1: Comparison between base case wind input 2020 and worst available wind year 2003. Visualising the KPI's for the segmented start strategy.

The outcome of the sensitivity case for the equal power division strategy is similar to segmented start, this is shown in figure 6.2. Again the annual hydrogen yield curve is similar, but achieves less yield overall. Consequently, the peak of the curve is at the same setpoint of 35% and the stable plateau starts at 67%. However, on average this situation achieves a 10% lower annual yield than the equal power division strategy in 2020.
Likewise, the outcome of the number of start-stop events is comparable to the outcome of the sensitivity case with the segmented start strategy. Namely, a steady increase in switching times until a setpoint of 30% and more start-stop events than the base-case scenario. Thereafter, there is a wobble around the maximum amount of switching time. The start-stop events increased on average by 7% in 2003. Analysing the average start-stop events per module, the first module consistently over setpoints experiences 120 switching times, the second module 270 and the third 279 times. Consequently, a module experiences 2%, 16% and 2% more start-stop events respectively throughout 2003.

The power fluctuation for this situation comes to an average power step of 0.62 MW and 5223 number of fluctuations for module 1, 1.06 MW + 2386 for module 2 and 1.43 MW + 1617 for module 3. Per module, compared to the base case this is an increase of 16%, 9% and 4% respectively. The total number of fluctuation occurrences increased by 12% for the year 2003. The operational hours of the modules also decreased compared to 2020 with 7%.

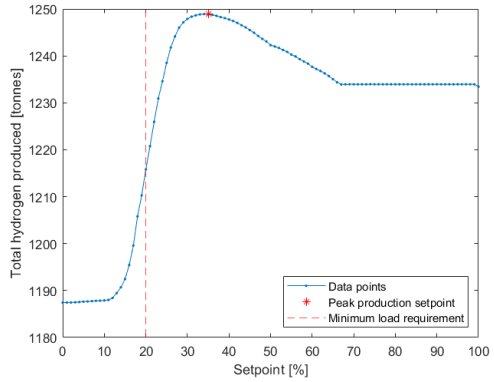

(a) Annual yield of H_2 for the segmented start strategy per variable setpoint for 2020.

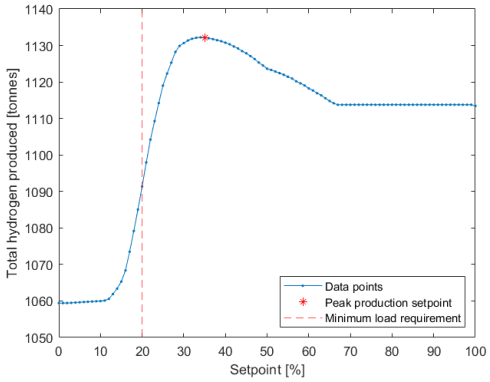

(b) Annual yield of H_2 for the segmented start strategy per variable setpoint for 2003.

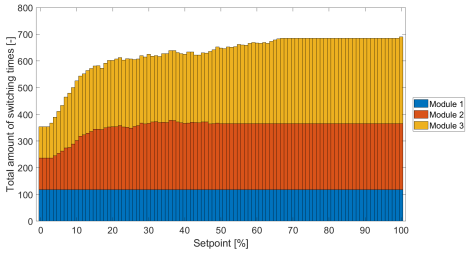

(c) Total number of switching times for the equal power distribution strategy per variable setpoint for 2020.

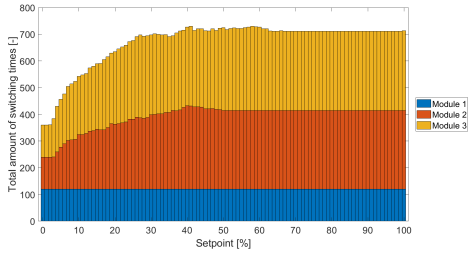

(d) Total number of switching times for the equal power distribution strategy per variable setpoint for 2003.

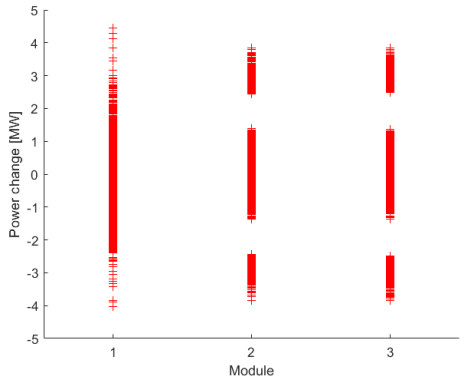

(e) Power fluctuation within the modules for a 3x 5MW configuration with the equal power division strategy and a setpoint of 50% for 2020.

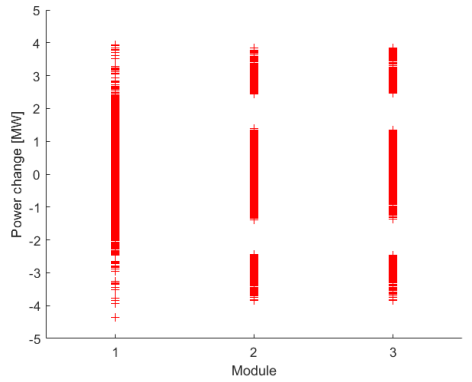

(f) Power fluctuation within the modules for a 3x 5MW configuration with the equal power division strategy and a setpoint of 50% for 2003.

Figure 6.2: Comparison between base case wind input 2020 and worst available wind year 2003. Visualising the KPI's for the equal power division strategy.

Both strategies experience the same decrease of 10% annual yield. This decrease results from lower wind speeds, which evidently comes from a less ideal wind year. Furthermore, the start-stop sequences for both situations increased by 7%, caused by the fact the wind speeds fluctuate more around the minimal required load to power the system sufficiently. However, how the two strategies cope with fluctuations is different per strategy. The segmented start strategy has a bigger increase in the number of fluctuations in poorer conditions compared to the equal power division, however compared to the

others, the segmented start still has a better performance on fluctuations.

6.2. Electrolyser sensitivities

Literature sources do not yet agree on a fixed required minimal load. They agree that a minimum load is required to prevent any cross-over risk. However, the minimum required load is different for each electrolysis technology. For example, the minimum required load is higher for alkaline than for PEM. During this study, a minimal load of 20% is determined to be a safe operational threshold for a PEM electrolyser (by Shell's internal sources). In literature and electrolyser specifications, two other thresholds are mentioned, specifically 5% and 10%. Therefore these two other cases will be analysed on the base case with the corresponding strategies.

With a lower minimal required load, a higher average annual yield is expected to be achieved. Because of a lower threshold, the system is able to start operating at lower wind speeds. Hence, as a result extending the operational range and achieving more yield. Furthermore, due to this lower threshold, less start-stop events are expected.
In the following figure, figure 6.3, the effect on the efficiency curve of lowering the minimal required load is displayed. It shows the three cases used in this sensitivity study. The biggest improvement from the base case is that the load range is extended. Accordingly, resulting in the effect that the module operates more. However, the peak efficiency also shifts to the left. This results in higher efficiencies in the lower operating range of a module and lower efficiency in higher partial load ranges.

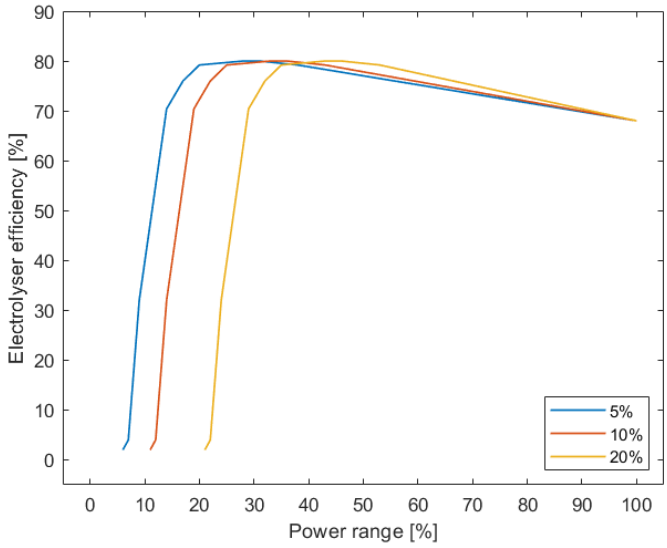

Figure 6.3: Efficiency curves for the PEM electrolyser. With minimal load criteria of 5%, 10% and 20%.

In table 6.1, the results on KPI's by means of a lower minimal required load is compared. In this table, average means the average taken across all setpoints. The improved percentage is relative to the base case (20%). It is evident from the table, that a lower minimal required load only improves the average annual yield for the segmented start strategy and does not affect the equal power division strategy on average. However, figure 6.4 shows the contrary and that the average is misleading in this scenario. This figure visualises the annual yield per setpoint for the base case and is followed by the sensitivity case of a lower minimal setpoint of 10 and 5%. From the first row of figures where the segmented start strategy is applied, it can be concluded that the setpoint where the peak yield is achieved stays at the same setpoint, but slightly decreases. The decrease in peak efficiency results from operating further away from the most efficient point on the efficiency curve.
When the system is operated on a selected setpoint and the aim is to achieve the highest yield, the annual yield will always be lower than the base case. For the segmented start strategy with a 10%

minimal required load, the peak value is decreased with less than 1% and for the 5% minimal required load the decrease in annual yield is 1%. Nevertheless, it is clear that at the less efficient setpoints a higher annual yield is obtained. The increase of annual yield in the low setpoint region, is the result of the lower minimal required load. From figure 6.4 a, b and c this effect is visible until the new threshold, so 20, 10 and 5% respectively. The higher annual yield in this region is mainly the reason why there is an increase in the average annual yield. Eventually, the increase in yield for the inefficient setpoint balances out the decrease in yield for the preferred setpoints.

The second row of figures in figure 6.4 illustrates that modifying the minimal load requirement impacts the annual yield for the equal power division strategy. The first observation is equal to segmented start, where in the lower setpoint region more yield is achieved. The next observation is the movement of the peak of annual yield, indicated with a red star. This point moves down and to the left, when decreasing the minimal required load. In other words, at lower setpoints, a lower peak yield is attained. Similarly, the decrease in peak efficiency results from operating further away from the most efficient point on the efficiency curve. However, with a larger operational window, a higher yield can be achieved at a lower setpoint, therefore the peak shifts to the left.
Comparing the influence on the peak values, the peak setpoint for annual yield shifts from 34% to 25% for the 10% minimal required load and to 21% for the 5% minimal required load. At these setpoints, the annual yield has decreased by less than 1% and 1% respectively. Consequently, the shift in the peak setpoint for annual yield results in a decrease in start-stop events. For the 10% case, a decrease of 2% is obtained and a 2% decrease for the 5% case.
For both strategies, the average number of power fluctuations is not much affected by the modification of the minimal load requirement. The reason for this is that in the low power region, which is now reached with a lower minimal required load, no additional power fluctuation exists.

From this sensitivity analysis, it can be concluded that a lower minimal required load does not result in an improvement in performance. The highest achievable annual yield is decreased. However, with a lower minimal required load the annual yield per strategy is more robust towards different setpoints. This points out that using a setpoint is highly recommended for the base case. The contrary result of the expectations is predominantly caused by the fact that with a lower minimal required load, the hydrogen production curve becomes similar to the power curve. Therefore, the input parameters like cut-in speed, the power capacity rating of the turbine and the high mean wind speeds have become more influential on the annual yield, the start-stop sequences and power fluctuations. Ultimately, using a minimal required load of 20% results in a safer operation and increases the annual yield.

	Average annual yield [tonnes H2]	**Average start-stop events**	**Number of fluctuations**
Segmented start - 20%	1173	213	6153
Segmented start - 10%	+1%	0%	0%
Segmented start - 5%	+2%	0%	0%
Equal power division - 20%	1228	207	8240
Equal power division - 10%	0%	0%	0%
Equal power division - 5%	0%	0%	0%
Confidential strategy - 20%	-	-	-
Confidential strategy - 10%	-	-	-
Confidential strategy - 5%	-	-	-

Table 6.1: Comparison of KPI's for different strategies with different minimal load requirements.

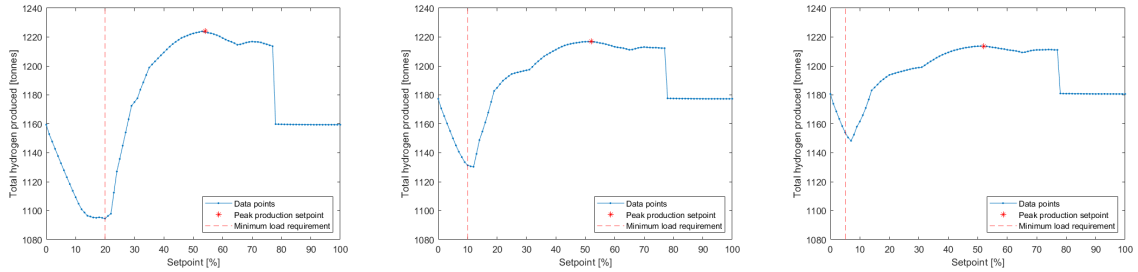

(a) Segmented start, base case (b) Segmented start, 10% (c) Segmented start, 5%

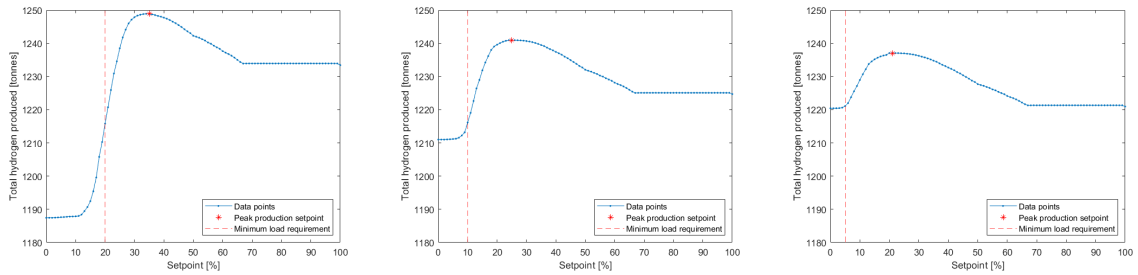

(d) Equal power division, base case (e) Equal power division, 10% (f) Equal power division, 5%

Figure 6.4: Overview of annual H_2 yield per setpoint, with modified minimal load requirement.

7

Conclusion

The goal of this study is to provide insight into the performance of an offshore hydrogen producing wind turbine, by analysing the effect of different control strategies and electrolyser dimensioning. The insights are created by defining a reasonable system configuration and selecting the most suitable components. The complete system is then translated into a mathematical model to simulate the coupling between wind energy and hydrogen production. The results from this model are evaluated by three key performance indicators. The annual hydrogen yield, the number of start-stop events and the number of power fluctuations determine if a strategy or configuration performs better. To provide adequate insights, three research questions are answered, which are concluded below.

The first research question assesses which power management strategy is the best fit for a hydrogen producing wind turbine. The results of this study show that each strategy performs best on its own objectives and therefore could be suited to a specific goal. Nevertheless, the equal power division strategy exceeded its expectations.
This study introduces three power management strategies, namely the segmented start strategy, equal power division and a confidential strategy. With the main goal of maximising annual hydrogen production, the equal power division strategy improves the yield by 5% compared to the segmented start strategy. This increase results from the modules operating at a lower partial load and therefore at a higher efficiency. In addition, this yield is achieved with 3% less start-stop events compared to the segmented start strategy. However, the equal power division strategy has the most number of power fluctuations. From literature and in-house knowledge, it is known that a start-stop event and power fluctuation speed up the cell performance degradation of electrolysers. When an electrolyser is directly coupled to an intermittent renewable energy source for green hydrogen production, it is essential to minimise these two effects. Nevertheless, because the effect is not quantified, it is hard to assess the impact. If the fluctuation drives the final decision, then the segmented start strategy is the preferred strategy. This strategy has the fewest number of fluctuations and scores moderately on the yield. However, it has the worst performance on start-stop events. If the focus is on achieving the least amount of start-stop events and therefore extending longevity, the confidential strategy is the best choice. This strategy's performance is moderate on power fluctuation and has the lowest yield.

The second research question is to analyse the effect of changing the total number of modules with the same capacity size. The base case of three modules of 5 MW each is adjusted to a single module of 15 MW and a six times 2.5 MW configuration. This study concludes that three times 5 MW is the best configuration in terms of KPI's.
The most significant changes are the hydrogen production at rated power and the minimum required wind speed for the system. With a larger number of smaller modules, the minimum wind speed required is reduced, but the hydrogen production at rated power is also reduced. With one big module, the minimum required wind speed increases and hydrogen production at rated power increases.
For the single module configuration, a power management strategy has no impact. This results in the lowest annual yield of all configurations, but also the lowest start-stop sequences and the lowest number of fluctuations.

In the case of the six times 2.5 MW configuration, applying a strategy with the right setpoint slightly increases the annual yield compared to the base case. However, independent of the setpoints, this configuration performs worse on degradation regarding the switching time and the number of power fluctuations.
In addition, there is no improvement in start-stop sequences per module when more modules are used in the configuration. Nevertheless, when considering the number of power fluctuations, the segmented start strategy with a six times 2.5 MW configuration experiences 28% less power fluctuation per module compared to the base case. While the experienced number of power fluctuations for the equal power division per module is 4% less. Ultimately, it is not recommended to use a 1x 15 MW or a 6x 2.5MW configuration.

The third research question investigates the impact of a different electrolyser capacity with a fixed wind turbine capacity. The two cases analysed are over-sizing with one additional module of 5 MW, adding to a total of 20 MW and under-sizing with the deduction of 5 MW to a total of 10 MW. The results demonstrate that reducing the capacity has no impact on the start-stop sequences of a module. Increasing the capacity does not influence the start-stop events of the first three modules either. However, the additional module is switched on and off more frequently in the first 55 setpoints, but the module is rarely used after this setpoint. Consequently, this module only contributes to an increase in yield in the first 55% of the setpoints. This phenomenon is the result of under-utilising the electrolyser modules and is the case for both strategies. The cases of over- and under-sizing in this study are no significant improvement to the base case. Therefore, adding or reducing a module is not recommended. However, there is a sweet spot in reducing the electrolyser capacity slightly. In this case, the electrolyser capacity should be equal to the available power of the system after powering the balance of plant.

To strengthen the results of previous conclusions, two sensitivity cases are studied. First, the base case is tested on a worse wind year to see how this influences the results. Secondly, the design parameter of the minimum load requirement of the electrolyser is modified to analyse the impact. In the first sensitivity study, it becomes clear that the influence of altering the setpoint stays the same despite the change in wind data input. The results show a decrease in annual yield and an increase in start-stop events and the number of power fluctuations, despite the robustness of the setpoint.
The second sensitivity analysis concluded that a lower minimal required load does not improve performance. Therefore, using a minimal required load of 20% results in safer operation and an increase in annual yield compared to the other cases. However, with a lower minimal required load, the yield is more robust towards different setpoints. Despite extending the operational range, the modules operate further away from the optimal partial load range, resulting in a lower annual yield. Nevertheless, this points out the benefits of using a setpoint in the base case.

This report shows that the use of a power management strategy improves the annual yield, but is also capable of minimising the effect of degradation caused by start-stop events and power fluctuation. This is an important development for improving green hydrogen production, as these strategies can be applied to multiple applications. The equal power division strategy increases the annual yield by at least 2%. The total number of power fluctuations can be significantly reduced by using the segmented start strategy. Finally, a strategy is developed to enhance the longevity of the system and diminish the degradation of the modules. Furthermore, it is recommended to use the three times 5 MW configuration. This configuration achieves the highest performance on the predetermined KPI's. In addition, over-sizing of the electrolyser capacity results in under-utilisation of the electrolyser. While under-sizing the electrolysis capacity leads to an increase in performance as the system is utilised more efficiently.

Recommendations and future work

The most significant recommendation for future work is to test and analyse the actual effect of start-stop sequences and power fluctuations on a module's efficiency. When the influence is clear and the degradation is quantified, a follow-up study can be performed. This study can use the results from this report and analyse over a longer period of time which strategy and configuration really does have the highest performance based on yield. Yield can now be the driver because the other two effects are accounted for in the efficiency. Furthermore, it can include the expected lifetime of a module and estimate the ideal time to replace a module.

Combined with the previous recommended study, a cost analysis could be included. Knowing a more accurate yield and the expected lifetime of a module, then the levelised cost of hydrogen (LCoH) can be calculated and optimised. With the LCoH and market value of a kilogram of hydrogen the most economically viable solution can be determined. This also gives a better insight into the most economical configuration of modules.

To gain improved insight, a more detailed model could be developed. This can be done in two ways. The more significant option is to step away from a high-level model and include a detailed electrolyser model based on the electrochemical process with temperature and pressure as drivers. With this implemented, more operational boundaries are used, providing more insights into the system's behaviour. Including this automatically involves the second way, namely modelling with smaller time steps. The current model runs on hourly data, however minutes to seconds will give a more detailed representation of the system. With smaller time steps, the influence of more variation becomes visual. For example, the ramping rate of the electrolyser and the modes within a start-stop cycle can be included.

A battery storage system could be added to improve green hydrogen production even further. This battery system can be implemented in the model for initial sizing. With an added battery system, the start-stop events and power fluctuation could be reduced. Furthermore, the power management strategies can be enhanced by charging and discharging the battery to improve performance. With a more detailed model, an additional study could be performed to optimise battery use with respect to hot and cold standby modes.

This study analyses the effect of three self-made power management strategies, however, the options for strategies are endless. An interesting strategy is when the setpoint can actively optimise itself. In this case, a strategy is not fixed on a setpoint, but can move around with a purpose. An option for this new strategy is to always optimise yield. To improve this new strategy, the model could implement wind speed prediction and weather forecasting. In this situation, the system is more resilient and can adapt to unprecedented situations. The enhancements are that start-stop sequences can be prevented and that big fluctuations can be easier divided.

An enhancement to this model is prioritising which electrolyser module to start first. Currently, it is based on a first on, last off principle. Whereby the first module always operates the most hours. To equally spread the degradation over the modules, a strategy could be implemented for the least degraded module to start first. This would result in a higher yield and evenly spread degradation, which leads to the convenience of swapping all the modules simultaneously, when necessary. It is therefore recommended to include this in a follow-up study.

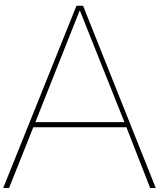

Confidential Appendix

B

Appendix B

Appendix B, is an extension to section 5.4. The hydrogen production over wind speed curves for the equal power division strategy are displayed in figure B.1 below.

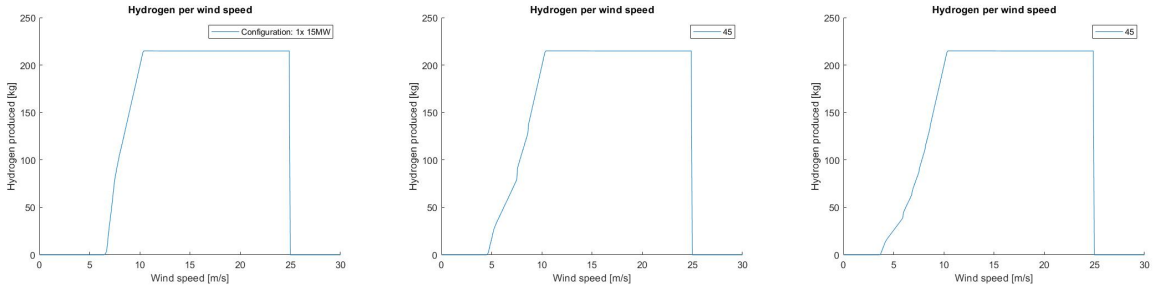

(a) 1x 15MW module configuration (b) 3x 5MW with equal start strategy (c) 6x 2.5MW with equal start strategy

Figure B.1: Hydrogen production curve over different wind speeds for the three different module configurations. For the last two figures, the equal power division strategy was selected.

The following figure, figure B.2, is a combination of the three curves shown in figure 5.13. They represent the three different configurations used. On the 3x 5 MW and the 6x 2.5 MW configuration, the segmented start is applied with a setpoint of 50%.

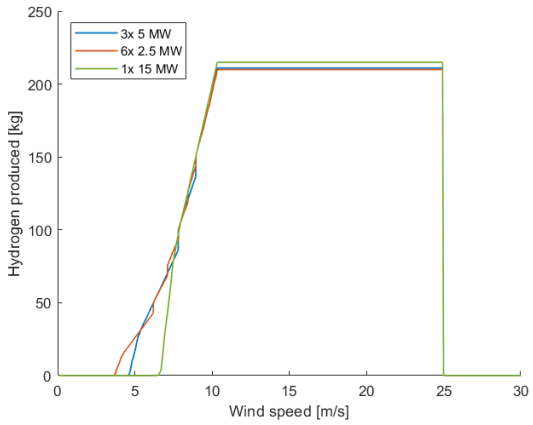

Figure B.2: Combination of hydrogen production curves over different wind speeds for the three different module configurations.

C

Appendix C

This appendix contains the figures which visualise the annual yield for the segmented start strategy and the equal power division strategy. In figure C.1, the first column contains the base case and the second column is the 6x 2.5 MW configuration. These figures have the same aligned axis for an easier comparison. It is evident that the equal power division with a 6x 2.5 MW configuration obtains the highest yield of all strategies.

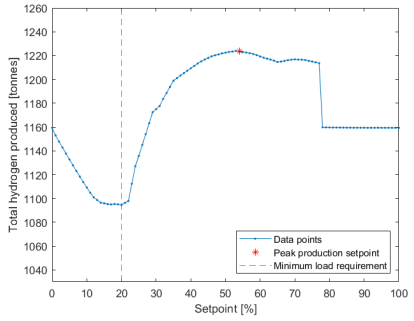

(a) Annual hydrogen yield for a 3x 5 MW configuration with segmented start strategy.

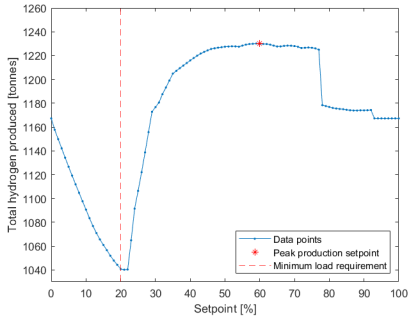

(b) Annual hydrogen yield for a 6x 2.5MW configuration with segmented start strategy.

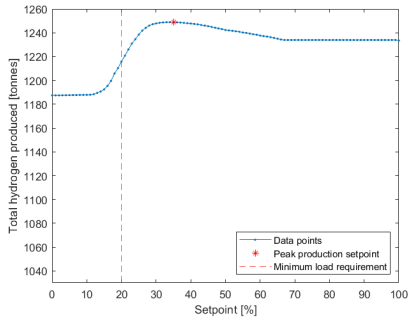

(c) Annual hydrogen yield for a 3x 5 MW configuration with equal power division strategy.

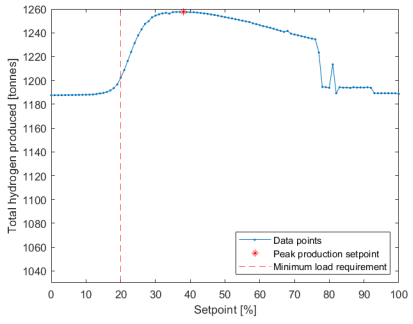

(d) Annual hydrogen yield for a 6x 2.5MW configuration with equal power division strategy.

Figure C.1: Comparing the effect on annual yield of different configurations and strategies.

Appendix D

This appendix covers the overruling high setpoint for equal power distribution. This part of coding is introduced because at high setpoints the equal power division would be highly inefficient. This effect is displayed in the following figure D.1.

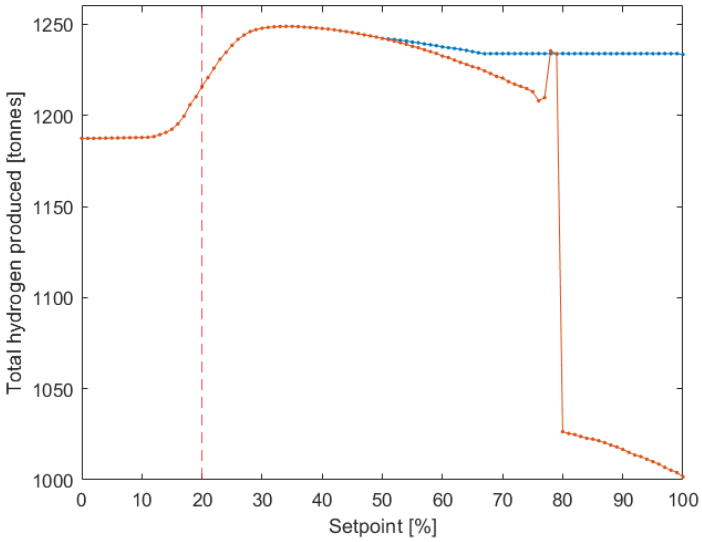

Figure D.1: Comparison of the annual yield between equal power distribution strategy with over-ruling setpoint code (blue) and without the improved code (orange).

Appendix E

This appendix shows the combination of over- and under-sizing of the segmented start strategy. The capacity difference between the two lines is 10 MW. The blue line is the 2x 5MW configuration where one module is deducted. The orange line is the 4x 5MW configuration with an added module.

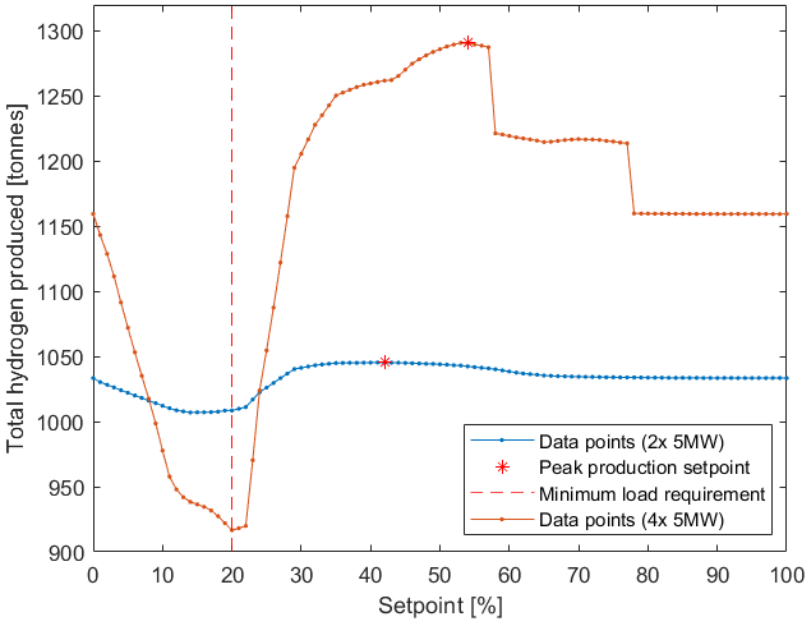

Figure E.1: Comparison of the annual yield of segmented start strategy comparing a 2x 5 MW and 4x 5 MW configuration.

Appendix F

This appendix discusses the potential layout of the system. For instance, a PEM Siemens Silyzer 300 unit with a 10 MW capacity would require an area of about 70 m^2, excluding 1.5 m at one side at least of the electrolyser for maintenance access, etc. (Jepma & van Schot, 2017) (North Sea Energy, 2018). In a simplified calculation, this means for a 15 MW electrolyser system, at least 105 m^2 is needed. Figure F.1, shows a very rough estimation for a possible system layout.

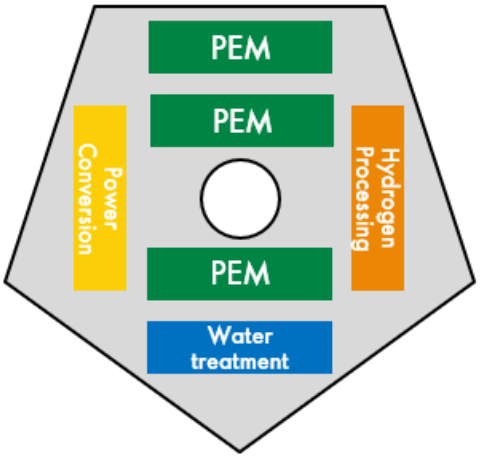

Figure F.1: Rough assumption of a possible system layout for an offshore decentralised electrolysis system integrated on a wind turbine platform.

Bibliography

Al-Karaghouli, A., & Kazmerski, L. L. (2013). Energy consumption and water production cost of conventional and renewable-energy-powered desalination processes. *Renewable and Sustainable Energy Reviews*, *24*, 343–356. https://doi.org/https://doi.org/10.1016/j.rser.2012.12.064

Ayodele, T., & Munda, J. (2019). Potential and economic viability of green hydrogen production by water electrolysis using wind energy resources in south africa. *International Journal of Hydrogen Energy*, *44*(33), 17669–17687. https://doi.org/https://doi.org/10.1016/j.ijhydene.2019.05.077

Buttler, A., & Spliethoff, H. (2018). Current status of water electrolysis for energy storage, grid balancing and sector coupling via power-to-gas and power-to-liquids: A review. *Renewable and Sustainable Energy Reviews*, *82*, 2440–2454. https://doi.org/https://doi.org/10.1016/j.rser.2017.09.003

Calado, G., & Castro, R. (2021). Hydrogen production from offshore wind parks: Current situation and future perspectives. *Applied Sciences*, *11*(12). https://doi.org/10.3390/app11125561

David, M., Ocampo-Martínez, C., & Sánchez-Peña, R. (2019). Advances in alkaline water electrolyzers: A review. *Journal of Energy Storage*, *23*, 392–403. https://doi.org/https://doi.org/10.1016/j.est.2019.03.001

ERM. (2019). *Dolphyn hydrogen, phase 1*. https://assets.publishing.service.gov.uk/government/uploads/system/uploads/attachment_data/file/866375/Phase_1_-_ERM_-_Dolphyn.pdf

Fernandes, D. (2020). Exploring p2h futures in the north sea using spatially explicit, techno-economic modelling. *Thesis TU Delft*.

Geerlings, J., & Mulder, F. (2021). Hydrogen technology. *SET3085*.

Ginsberg, M. J., Venkatraman, M., Esposito, D. V., & Fthenakis, V. M. (2022). Minimizing the cost of hydrogen production through dynamic polymer electrolyte membrane electrolyzer operation. *Cell Reports Physical Science*, *3*(6), 100935. https://doi.org/https://doi.org/10.1016/j.xcrp.2022.100935

Guo, Y., Li, G., Zhou, J., & Liu, Y. (2019). Comparison between hydrogen production by alkaline water electrolysis and hydrogen production by pem electrolysis. *IOP Conference Series: Earth and Environmental Science*, *371*(4), 042022. https://doi.org/10.1088/1755-1315/371/4/042022

Hernández-Gómez, Á., Ramirez, V., & Guilbert, D. (2020). Investigation of pem electrolyzer modeling: Electrical domain, efficiency, and specific energy consumption. *International Journal of Hydrogen Energy*, *45*(29), 14625–14639. https://doi.org/https://doi.org/10.1016/j.ijhydene.2020.03.195

Ibrahim, O. S., Singlitico, A., Proskovics, R., McDonagh, S., Desmond, C., & Murphy, J. D. (2022). Dedicated large-scale floating offshore wind to hydrogen: Assessing design variables in proposed typologies. *Renewable and Sustainable Energy Reviews*, *160*, 112310. https://doi.org/https://doi.org/10.1016/j.rser.2022.112310

IEA. (2022). *Global hydrogen review 2022*. Retrieved December 24, 2022, from https://www.iea.org/reports/global-hydrogen-review-2022

IRENA. (2018). Hydrogen from renewable power technology outlook for the energy transition. https://www.irena.org/-/media/files/irena/agency/publication/2018/sep/irena_hydrogen_from_renewable_power_2018.pdf

IRENA. (2020). Green hydrogen cost reduction, scaling up electrolysers to meet the 1.5c climate goal. https://irena.org/-/media/Files/IRENA/Agency/Publication/2020/Dec/IRENA_Green_hydrogen_cost_2020.pdf

Jepma, P. C. J., & van Schot, M. (2017). On the economics of offshore energy conversion: Smart combinations. converting offshore wind energy into green hydrogen on existing oil and gas platforms in the north sea. *Energy Delta Institute*.

Khan, M. A., Al-Attas, T., Roy, S., Rahman, M. M., Ghaffour, N., Thangadurai, V., Larter, S., Hu, J., Ajayan, P. M., & Kibria, M. G. (2021). Seawater electrolysis for hydrogen production: A solution looking for a problem? *Energy Environ. Sci.*, *14*, 4831–4839. https://doi.org/10.1039/D1EE00870F

Kopp, M., Coleman, D., Stiller, C., Scheffer, K., Aichinger, J., & Scheppat, B. (2017). Energiepark mainz: Technical and economic analysis of the worldwide largest power-to-gas plant with pem electrolysis [Special Issue on The 21st World Hydrogen Energy Conference (WHEC 2016), 13-16 June 2016, Zaragoza, Spain]. *International Journal of Hydrogen Energy*, *42*(19), 13311–13320. https://doi.org/https://doi.org/10.1016/j.ijhydene.2016.12.145

Madariaga, A., de Ilarduya, C. J. M., Ceballos, S., de Alegría, I. M., & Martín, J. (2012). Electrical losses in multi-mw wind energy conversion systems. *European Association for the Development of Renewable Energies, Environment and Power Quality (EA4EPQ)*.

May, T., Yeap, Y. M., & Ukil, A. (2016). Comparative evaluation of power loss in hvac and hvdc transmission systems, 637–641. https://doi.org/10.1109/TENCON.2016.7848080

Mehta, M., Zaaijer, M., & von Terzi, D. (2022). Optimum turbine design for hydrogen production from offshore wind. *Journal of Physics: Conference Series*, *2265*(4), 042061. https://doi.org/10.1088/1742-6596/2265/4/042061

Miao, B., Giordano, L., & Chan, S. H. (2021). Long-distance renewable hydrogen transmission via cables and pipelines. *International Journal of Hydrogen Energy*, *46*(36), 18699–18718. https://doi.org/https://doi.org/10.1016/j.ijhydene.2021.03.067

Nejad, A. R., Keller, J., Guo, Y., Sheng, S., Polinder, H., Watson, S., Dong, J., Qin, Z., Ebrahimi, A., Schelenz, R., Gutiérrez Guzmán, F., Cornel, D., Golafshan, R., Jacobs, G., Blockmans, B., Bosmans, J., Pluymers, B., Carroll, J., Koukoura, S., … Helsen, J. (2022). Wind turbine drivetrains: State-of-the-art technologies and future development trends. *Wind Energy Science*, *7*(1), 387–411. https://doi.org/10.5194/wes-7-387-2022

North Sea Energy. (2018). *Towards sustainable energy production on the north sea - green hydrogen production and co2 storage: Onshore or offshore?* Retrieved October 8, 2022, from https://north-sea-energy.eu/static/fc2fba594593abe1330f8b80eeaad756/NSE1_D3.6-Towards-sustainable-energy-production-on-the-North-Sea_final-public.pdf

NREL. (2020). *Definition of the iea wind 15-megawatt offshore reference wind turbine*. Retrieved September 12, 2022, from https://www.nrel.gov/docs/fy20osti/75698.pdf

Rijksdienst Voor Ondernemend Nederland. (2021). *Memo "minimum last, stop/start en degeneratie van elektrolysers"*. Retrieved December 21, 2022, from https://www.rvo.nl/sites/default/files/2022/01/2021-12-Memo-minimum-last%20stop_start-en-degeneratie-van-elektrolysers.pdf

Santos, D. M. F., Sequeira, C. A. C., & Figueiredo, J. L. (2013). Hydrogen production by alkaline water electrolysis. *Materials Electrochemistry Group*.

Schnuelle, C., Wassermann, T., Fuhrlaender, D., & Zondervan, E. (2020). Dynamic hydrogen production from pv & wind direct electricity supply – modeling and techno-economic assessment. *International Journal of Hydrogen Energy*, *45*(55), 29938–29952. https://doi.org/https://doi.org/10.1016/j.ijhydene.2020.08.044

Siemens-Energy. (2020). *Datasheet silyzer 300*. Retrieved September 26, 2022, from https://assets.siemens-energy.com/siemens/assets/api/uuid:a193b68f-7ab4-4536-abe2-c23e01d0b526/datasheet-silyzer300.pdf?ste_sid=7507737a9e6fa6fbc90e2b4756a89c88

Siemens-Energy & Lettenmeier, P. (2021). *Efficiency–electrolysis*. Retrieved September 27, 2022, from https://assets.siemens-energy.com/siemens/assets/api/uuid:a193b68f-7ab4-4536-abe2-c23e01d0b526/datasheet-silyzer300.pdf?ste_sid=7507737a9e6fa6fbc90e2b4756a89c88

Siemens-Gamesa. (2021). *Green hydrogen, fuel for the future*. Retrieved October 3, 2022, from https://www.siemensgamesa.com/products-and-services/hybrid-and-storage/green-hydrogen

Singlitico, A., Østergaard, J., & Chatzivasileiadis, S. (2021). Onshore, offshore or in-turbine electrolysis? techno-economic overview of alternative integration designs for green hydrogen production into offshore wind power hubs. *Renewable and Sustainable Energy Transition*, *1*, 100005. https://doi.org/https://doi.org/10.1016/j.rset.2021.100005

Turner, J. A. (2004). Sustainable hydrogen production. *Science*, *305*(5686), 972–974. https://doi.org/10.1126/science.1103197